WP4–Human factors simulation in BETs and definition of a related behavioral-based (B-based) resilience metric

T4.1 Development of simulation model including human behavior representation and BETs modifications for selected SLOD/SUOD

DELIVERABLE ID	D4.1
Deliverable Title	selected SLOD/SUOD simulation tool for BETs delivered
Delivery month	M18
Revision	1.2
Main partner	UNIVPM
Additional partners	POLIMI, UNIPG
Authors of the contribution	Gabriele Bernardini (UNIVPM); Enrico Quagliarini (UNIVPM); Marco D'Orazio (UNIVPM); Juan Diego Blanco Cadena (POLIMI); Martha Caramia (POLIMI); Graziano Salvalai (POLIMI); Federica Rosso (UNIPG); Letizia Bernabei (UNIPG); Giovanni Mochi (UNIPG)
Deliverable type	report
Number of pages	46

Abstract

Simulation models can effectively support risk and resilience assessment in the Built Environment (BE) if they can evaluate the interactions between the BE users and the BE features, its possible hazards and the effects of such hazard on the BE itself. Thus, representing users' exposure (in terms of number of people in the BE) and vulnerability (in terms of users' types and behaviours) is a key factor to reach this goal. This deliverable starts from this approach and develops a combined simulation models according to an agent-based methodology, so as to effectively represent the features and the rules aiming each individual receptor at risk, as well as the mutual interactions. The model shares a unique architecture based on the NETLOGO platform, which also adopts a microscopic approach to simulate the BE users' behaviours. The same architecture is adopted to set up the BE, by taking advantages of the BE Typologies (BETs) characterization in T3.1 and T3.2. Using BETs allows tracking the key factors characterizing the BE under examination in this work, as well as the specific risk-affecting factors. The users move in the BE according to a microscopic (i.e. Social-Force Model) approach, that can represent each individual features (including age, gender, motion abilities and so on) and behaviours in respect to the BET elements (i.e. depending on their characterization and selection given in D3.2.1) and the BET modifications due to the specific SLOD/SUOD (i.e. depending on the results of D3.2.2). Thus, specific algorithms are included to represent terrorist acts, earthquake, heat waves and pollution, according to the experimental results of WP1 and WP2. The exposure quantification is derived according to the typological analysis in D3.2.3. Simulations are organized to evaluate each risk in a separate manner for each BET, thus demonstrating the model capabilities and providing basic validation according to the experimental results of WP1 and WP2. Then, some basic key metrics (e.g. evacuation times for SUODs; exposure

time for SLODs), are defined, being the bases for T4.2 activities on the behavioural-based metrics development.

Keywords

Users' typical exposure; Individual vulnerability; Human exposure; factors characterization;

Approvals

Role	Name	Partner
Coordinator	Enrico Quagliarini	UNIVPM
Task leader	Enrico Quagliarini	UNIVPM

Revision versions

Revision	Date	Short summary of modifications	Name	Partner
0.1	04.04.2021	SLOD and SUOD simulator integration (sections 3.1 and 4.1)	Blanco Cadena Rosso	POLIMI UNIPG
1.0	27.09.2021	Model description integration	Bernardini Blanco Cadena Rosso	UNIVPM POLIMI UNIPG
1.1	15.06.2022	Integration on results according to the evacuation software improvements	Bernardini	UNIVPM
1.2	18.12.2022	Appendix B final integration within the document	Bernardini	UNIVPM

Summary

1. Introduction: BET-related simulations for resilience assessment

According to a behavioural-based perspective, the Built Environment (BE) risk and resilience should be based on the joint representation of the BE features, the hazards effects on the BE and the users' reactions to the disaster conditions (Bernardini et al. 2016a). Then, simulation modes should be developed to this end by pursuing probabilistic and microscopic approaches (Ronchi et al. 2014; Kuligowski 2016; Lumbroso and Davison 2018). In this case, reasoning on the BE Typologies (BET) could be more effective than testing single scenarios, since their recurring conditions can be assessed in a more feasible way (Bernardini et al. 2021).

Due to the configuration of the BET (see D3.1.1 and D3.2.1) and to the nature of the Hazard pursued by the BE S2ECURe project (see D3.2.2), the simulation should be mainly related to the Open Spaces in the BE, that are the outdoor area surrounding by the Continuous Built Fronts (CBF) (Sharifi and Lehmann 2015; Sharifi 2019a, b; Russo et al. 2020; Quagliarini et al. 2021a). In fact, the interactions between the users and the BE are mainly relevant in the outdoor scenario, as also remarked by experimental-based analysis of D1.2.5, D1.3.3 and D2.2.3, because: 1) in seismic risk (SR), outdoor evacuation is highly affected by the damage levels, given by the debris; 2) in terrorist acts risk (TR), people in outdoor spaces can be more exposed to the different types of attacks; 3) in both SLODs, that are heat waves (HR) and pollution (PR), people in outdoor are more exposed than people remaining inside the buildings.

The Netlogo platform (Wilensky 1999) could be useful to describe microscale interactions between each receptor at risks, since it adopts an agent based modelling approach (Almeida et al. 2012; Chu et al. 2015; Simeone et al. 2016; van der Wal et al. 2021). Each agent "On the scene" is characterized by a series of rules and individual features, and the overall effects of the agent-agent interactions lead to the macroscale effects noticed in experimental conditions (Parisi and Dorso 2005). The main advantages of Netlogo use are the freeware and opensource access to the platform (as well as to many different previously developed codes), the well-established features and functions for accurate modelling of different agents' behaviours, and the possibility to easily replicate the experiments to derive different scenarios and their variations (Wilensky 1999; Wilensky and Rand 2015).

Different evacuation models were developed according to the Netlogo platform (Camillen et al. 2009; Almeida et al. 2012; Mas et al. 2013; Pluchino et al. 2015). Available examples of microscopic modelling of users' motion in the BE according to the Social Force Model (Helbing and Molnár 1995) exist, e.g.: http://modelingcommons.org/browse/one_model/4300#model_tabs_browse_procedures and https://github.com/chraibi/SocialForceModel (last access: 14/04/2021). The Social Force Model approach ensures evaluating the interaction of the users in a continuous plane, whose boundary conditions for the BE representation only depend on the grid dimension. Thus, trajectories can be also clearly outlined in both normal and emergency conditions. In emergency conditions due to a SUOD, this approach has a good computing costs-simulation benefits ratio, since the simulation times are quite small (ideally, some minutes according to the users' reaction timelines to reach a safe area) (Opper et al. 2010).

Starting from these basic points, this work provides a Netlogo-based simulation model for SUOD and SLOD assessment in the BETs, by representing the BETs users' behaviours. The model can be used to both simulate the selected BET conditions, as well as specific BEs according to the same criteria. Then, we used the notation "BE(T) simulation" to point out this kind of capabilities of the simulator.

2. Methodology and phases

The work is organized in the following phases. Firstly, the model architecture is defined (Section 2.1), according to an Agent-Based Model approach. This section also points out the dependency between the SLOD conditions and the SUOD conditions, according to Annex to D2.2.5. Then, the basic BET matrix is defined (Section 2.2), to define the elements to be included in the built environment representation. Rules for users' representation are also assessed (Section 2.3) depending on SUOD/SLOD-related specific behaviors, as also described in D1.2.5, D1.3.3 and D2.2.3 and their integration. Finally, the basic metrics for output analysis are also defined (Section 2.4).

2.1 Overall model architecture

The architecture shown in Figure 1 is based on three main agents (Wilensky and Rand 2015): (1) the physical BE(T), described according to D3.2.1 results; (2) the hazard features, described according to D3.2.2, Section 4 and Section 9; (3) the users' features, derived from D3.2.3 results. Figure 1 resumes the interaction scheme between the agent in a general manner. The users move in the BE(T) by interaction with their main elements, and by interacting one each other. Hazard conditions alter the users' motion by provoking specific response behaviors since the hazard modifies the BE(T) features.

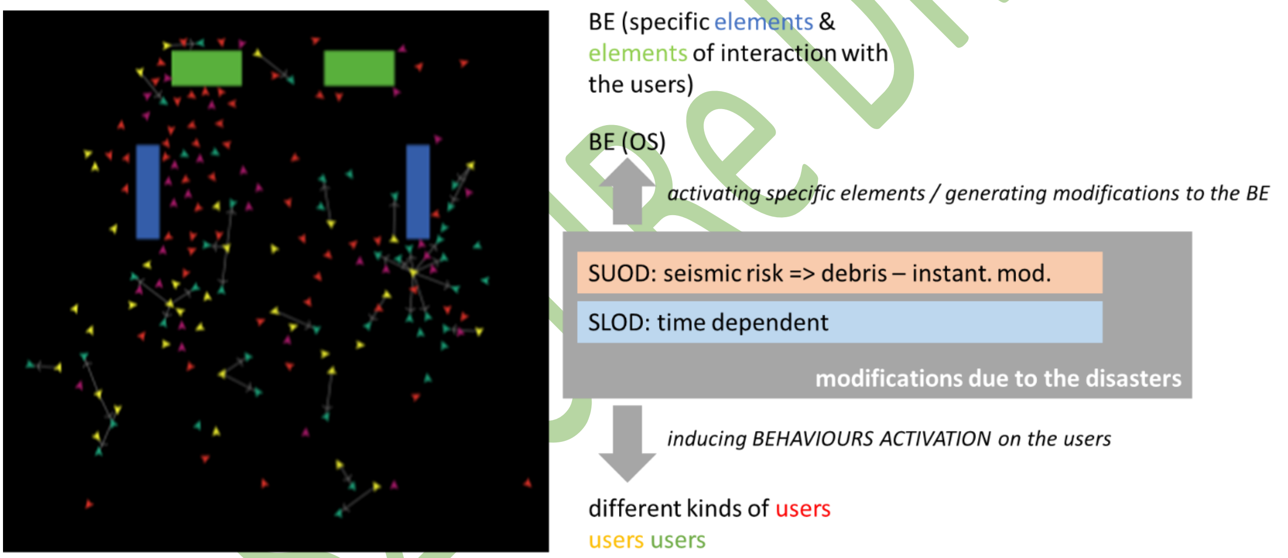

Figure 1. General schematization of the simulation model, by mainly pointing out the agents, their relation and the time-related issues. Left: Netlogo image from http://modelingcommons.org/browse/one_model/4300#model_tabs_browse_nlw (last access: 30/04/2021).

The users' generation in the scenario is the fundamental element in the architecture of the model, since it represents the interaction between them and the BE(T)/its conditions at the starting of the simulation. Firstly, the users' position is considered depending on the BE(T) area uses, as better assessed by following Section 2.2. In addition, specific strategies in simulation depending on SLOD, SUOD and combined SLOD-SUOD conditions should be considered as follows. For SLODs, modifications are time dependent and should involve a longer period than SUODs (e.g. some hours). The identification of peaks in the risk conditions can lead to assume the analysis of short time periods, although seasonal simulation, and daily simulation can be performed, e.g. estimating the overall (including daily) exposure levels of pedestrians and residents by assuming simplified dynamics in the users' permanence inside the spaces and motion issues (Blanco Cadena et al. 2021). For the generation of people in a SLOD, conditions referring to heatwaves and their risk matrices (HRM) are assumed according to the risk combinations as in D3.2.2, since they have a direct impact on the users' presence in the outdoor use. In fact, the outdoor conditions, in terms of air temperature, or UTCI or PET, are able to impact the acceptability to maintain a certain position in the BE(T) because they can stress the users while moving or staying in it for a longer time (Paolini et al. 2014; Jamei et al. 2016; Cheunga and Jim 2019). Once the users' position is assessed, the SLOD simulation can be performed by recursively assess the probable position of people in the BE(T) depending on such conditions. In this sense, a simulation steps of an adequate duration should be defined. This strategy can be used to investigate HRM by itself as well as its combination with Pollution (PRM) stressors, as in D3.2.2.

For SUODs, modifications are considered as instantaneous, thus the simulation timing is related only to the evacuation process, e.g. some minutes up to one hour (D'Orazio et al. 2014). In particular, the work assumes no building-related modifications for terrorist act inducing damage to the open spaces. Populating the scenario with users means to randomly locate them in the space depending on the BE(T) area uses (which also define their ideal density), and to the time of the day or kind of day (i.e. working, holiday) considered for the simulation.

The rationale for the SUODs simulation depends on the type of emergency, thus dividing the earthquake risk and the terrorist act risk in view of their specificities relating to the evacuation process in the urban context (Li Piani 2018; Shrestha et al. 2018; French et al. 2019; Quagliarini et al. 2021a). However, in both the scenarios, given T0 as the moment of the emergency raising, simulations consider the immediate response to the emergency by the occupants (T1), and not the aftermath, in which people from other areas in the urban fabric can move towards the BE(T) or from it (T2) (Villagràn De León 2006).

During an earthquake emergency, the users into the square will remain in it because it represents the first available wider space in the urban fabric, while the users from the access streets will try to move into the square especially if the access streets have a limited width (Bernardini et al. 2019). Two simulation approaches can be considered.

The first simulation approach implies the evacuation simulation. The users from the access streets will ideally have a significant impact if the crowding level along them will be significant, that is if the intended uses hosted in the buildings along them will generate wide Space of Relevance SoR (Li Piani 2018) interfering with the square space itself (see also D3.2.3, Section 4.1 for the interference evaluation). As a consequence, users' flows will enter the BE(T) from the access streets, ideally at maximum flow that is the ones relating to pedestrian's density of about 2pp/m^2 (ranging from about 1.5pp/s for general motion purposes to about 2.5pp/s for specific earthquake conditions) (Bernardini et al. 2016b; Banerjee et al. 2018). These flows can be considered as ideally distributed between the different accesses to the BE(T). In case no interfering SoR is noticed, flows will be equal to zero. In such conditions, simulations will be overlooked and only two kinds of combined geometry and damage-based analysis will be performed: (a) the area of the BE(T) free of debris will contain the overall number of users without critical density-based interferences (e.g. 3pp/m^2 while waiting for rescuers' arrival) (Zlateski et al. 2020); (b) depending on the debris dimension at the access streets, a sufficient free-of debris width can ensure the access of rescuers' vehicles (at least 3.5m (Italian Government 1996)) or the users' passage to leave the BE(T) (at least 1m).

The second simulation approach adopts a quick-to-apply overview that just would like to consider the ratio between the autonomous users' number (including people in the BE(T) and in the surrounding streets) and the area that is free-of-debris (Zlateski et al. 2020). The area of the BE(T) free of debris should contain the overall number of users without critical density-based interferences (e.g. 3pp/m^2 while waiting for rescuers' arrival). In this sense, there is no simulation of the evacuation process, but just the analysis of final effects. This work pursues this second approach, due to the application rapidity.

The terrorist act is considered as occurring into the BE(T), that is in the square itself, so as to maximize the number of exposed users. Therefore, users will leave the square, moving towards the access streets and thus evacuating the BE(T) (FEMA-426/BIPS-06 2011; Liu 2018). In this case, the users from the SoR (if present) will be considered into the space of the BE(T) to increase the number of exposed users, thus considering that they are passers-by (or rather Only Outdoor – OO users, as in D3.2.3, Section 4.1) using the square space to move from/towards the intended uses placed in the access streets.

Finally, for SLOD-to-SUOD combination, the approach can define the occurrence of SUOD conditions under previous SLOD situation. Thus, HRM conditions are used to populate the starting of the SUOD simulation. Then, the SUOD simulation can be performed according to the evacuation process evaluation.

2.2 Basic BET matrix representation in the simulation model in view of the Netlogo implementation

Table 1 resumes the BET variables.

Global variables are identified as unique elements for the whole BE(T). This choice fits with the homogenous definition of BET conditions, especially concerning vulnerability-related aspects against SUODs and SLODs.

"Patches" refers to the single tiles within the simulation environment representing the BE(T). The ideal patch dimension can be organized according to a 0.35m side length (squared patches), into a simulation grid defining the BE(T) (Almeida et al. 2012). This solution will allow to set up the motion space according to the users' dimension. Nevertheless, patches having a greater dimension are allowed too, but the geometry will re-scale it according to the 0.35m grid. These patches can be described according to a colour-based approach or by specific attributes (patches-own) that represent additional layer for the BE(T) characterization (Wilensky and Rand 2015). This choice ensures a rapid implementation of the BE(T) conditions into NETLOGO as well as a rapid possibility to visualize inputs and results, according to a cellular automata (CA)-based approach too (Li et al. 2018; van der Wal et al. 2021; Hassanpour and Rassafi 2021).

"Breed" elements are described as specific "turtles", or rather punctual agents (Wilensky 1999).

Table 1. Parameters of the BE(T) for the model implementation in Netlogo. TBD: to be decided; n.a.: not assessed at the current time

Agent	Resources	Modelling representation as INPUT data	Scale	Attributes [unit of measure]; NetLogo type	Time dependent	Source from D3.2.1	Main Source from D3.2.2
BUILT ENVIRONMENT	Geometry	2D model to define buildings (not walkable spaces) and the Open Space area (walkable spaces)	patches	debris [m]; patches-own		P1+P2+P8	
	Green	green area, including trees, bushes and grass as possible obstacles and/or attractor for users' motion	patches	modelled as coloured patches + greenery [m]; patches-own		P9	
	Attraction poles	describing the patches as attractors for the users' movement, by distinguishing between: (1) building entrances; (2) special uses in the BE and/or sights; (3) safe areas in emergency conditions for SUODs	patches	n.a. [m]; just modelled as coloured patches depending on the type of attraction, mainly characterized as width/ overall dimension as number of patches		including P5	S4_3.1 (special uses in the BE) + S4_7.1 (sights)
	Accesses	describing the entrances and exits from the Open Space, which can be used to reach the BE by the users, or to	patches	n.a. [m]; just modelled as coloured patches, mainly characterized as width as number of patches		P4	S2_F_2
	Porticoes **(optional)**	shaded areas for SLODs, which attract the users	patches	n.a. [m]; just modelled as coloured patches, mainly characterized as		P7	

		during their motion and permanence		overall dimension as number of patches			
	Areas for vehicles	spaces that people can cross but cannot use for the permanence during normal fruition conditions (i.e. in SLODs), while become a walkable area for SUODs	patches	n.a. [m]; just modelled as coloured patches, mainly characterized as width/ overall dimension as number of patches			S4_4 + S4_7
	Emergency facilities **(optional)**	attractors for the evacuation process, e.g. wayfinding signage, as well as counter-SLODs measures, e.g. canopies; they are "turtles" that cannot move during the time	breed	they can be included in retrofitted BET (according to D5.1.1 criteria)			
HAZARD	Constructive characteristics + SRM	2D model where damage occur depending on the effects of Seismic intensity on a given constructive characteristics of the CBF	patches	debris [m]; patches-own, just included as input in the simulation		P3	S5_1.1
	HRM and its combinations	UTCI	patches	temperature [°C]; patches-own, just included as input in the simulation for the probable positioning of users	x		S5_3.3

	PRM	Pollutant concentration[1]	patches	Pollutant concentration [AQ]; patches-own	x		S5_3.6

[1] This issue will be not considered in the final simulation model for behavioural effects, but just in the input data for KPIs assessment. Compare with Section 3.1 and D4.2.3.

2.3 Rules for users' representation in view of the Netlogo implementation

2.3.1 General rules: users' typology and main possible behaviors

Six types of agents are modelled depending on their specific age-related typologies, which influence their motion speed and abilities (Shi et al. 2009; Bosina and Weidmann 2017), also according to D3.2.3 outcomes (Section 6.1):

1. toddlers **TU** from 0 to 4 years, who directly depends on their parents to move in the BE;
2. parent-assisted children **PC** from 5 to 14 years, who can autonomously move but are generally strictly influenced by their parents' use of the BE;
3. young autonomous users **YA** from 15 to 19 years, who can be considered as autonomous users of the BE, but scholars;
4. adult users **AU** from 20 to 69 years, who can be considered as autonomous users of the BE, but potentially workers;
5. elderly **EU** from 70 to 100+ years, who can have a reduced use of the BE with respect to the AU.
6. disabled people, so as to outline disabilities in motion which are not associated to one of the previous categories

In addition, the "staff" agents, which can described all the rescuers, are modelled as the type "adult" (Ji and Gao 2007; Gayathri et al. 2017). They can support people in emergency conditions (van der Wal et al. 2021).

Furthermore, the model distinguishes between residents and non-residents users, according to the percentage values in D3.2.3 (section 6.1), so as to point out differences in terms of familiarity with the built environment (Li and Klippel 2016; Quagliarini et al. 2021b). Gender differences are also introduced according to D3.2.3, Section 6.1.

In general terms, it is assumed that agent can follow different rules depending on the hazard considered in the BE(T) simulation. These rules lead them to move towards a certain direction or stop in a particular part of the BE(T), by mainly distinguishing between:

- "**move-to-building**": people will move from a point of the BE(T) to a building, in the SLOD simulation and in normal fruition time. The building selection can be assessed in a random way
- "**move-to-access**": people will move from a point of the BE(T) to one of the exit, in the SLOD simulation and in normal fruition time. The access selection can be assessed in a random way
- "**evacuate**": people will move towards the safe area, in SUODs conditions
- "**move-to-shadow**": people will change their direction to mainly move towards and under shaded areas, in SLOD conditions

In particular, the simulator development will consider the "evacuate" behaviours for SLOD-to-SUOD simulation according to an affordance-based approach (Nasir et al. 2014; Liu et al. 2016; Hassanpour and Rassafi 2021). According to its original definition (Mayzner et al. 1978; Hartson 2003), each element in the built environment (and so each part of it) can support an agent in doing an action thanking to its features, and considering different levels of interaction. In a CA perspective, each cell representing the outdoor space in the BET can be represented by different features leading the individual to use it while moving. This approach consider that each pedestrian will try to maximize his/her motion direction towards a safe area by using a certain path (and so a certain groups of cells) depending on the combination between distance to the evacuation goal, crowd conditions, risk conditions and other factors of interactions with buildings (i.e. distance from the buildings for safety purposes, especially in earthquake evacuation). Equation 1a resumes the concept of cell *c* affordance at a given time *t* Aff_{it} [-], which ranges from 0 to 1 according to the definition of its specific factors, according to reference works by (Liu et al. 2016), as well the calculation of the composing normalized factors $f_{c,}t$ (see Equation 1b) staring from the local cell conditions $f_{c,t,input}$ that are:

- $P_{i,c,t}$ [-] is the normalized impact of crowd conditions near the cell *c* according to the extended Moore neighborhood approach (Hassanpour and Rassafi 2021). Firstly, $P_{i,c,t}$ is calculated for the cells occupied by an individual, and it is based on the number of other people placed at a radius equal to the distance that this individual could reach at his/her current speed within a reaction time of 1s. Then, the pedestrians' density is calculated diving this value by the number of cells that are not obstacles (e.g. buildings, monuments,..) for the individual motion;
- $F_{d,c,t}$ [-] is the normalized impact of distance calculated by in reference to the closest safe area in the BET. The distance of a specific cell $F_{d,c,t,input}$ is calculated according to the Standard Priority Queue Flood Fill Algorithm[2]. A visibility factor is introduced to increase the distance of the cell from the safe area when there is no visibility due to an obstacle (i.e. buildings, monuments) obstruction in the field of view. The same visibility factor is applied to dehors areas so as to permit users to leave them but not using them unless they are located along the evacuation path to the safe area;
- $R_{c,t}$ [-] is the normalized impact of risks in the BET open space, such as those due to cascading effects in SUODs (e.g. fires after earthquakes) or to their direct effects which can remain over the time (e.g. snipers' shot/knife attack areas in terrorist acts). It could be also used to simulate earthquake debris impact on the path selection, too;
- $OR_{c,t}$ [-] is the normalized impact of distance from buildings and high obstacles, due to "feel of high obstacles" during earthquakes (Bernardini et al. 2019). In this case, a maximum value conditions of 3meters is assumed (Lakoba et al. 2005).

$$Aff_{\ c,t}[-] = \alpha P_{i,c,t} + \beta F_{d,c,t} + \gamma R_{c,t} + \delta O_{c,t} \quad \text{(Eq. 1a)}$$

$$f_{c,t}[-] = \left(f_{c,t,input,max} - f_{c,t,input}\right) / \left(f_{c,t,input,max} - f_{c,t,input,min}\right) \quad \text{(Eq. 1b)}$$

Finally, the corrective coefficients in Equation 1a allow scaling the importance of each normalized factors, thus varying from 0 to 1. For instance, if only $\beta = 1$, the shortest evacuation path selection is used by pedestrians to move towards the safe areas in the BET (Liu et al. 2016; Hassanpour and Rassafi 2021).

2.3.2 Specific rules for users' representation depending on SLOD/SUOD

According to Section 2.1, the first rule for users' representation concerns their generation in the BE(T). D3.2.3 results (i.e. Section 6.1) are used to define:

- **the overall users' number**, which depends on the time of the day (distinguishing between working day, holiday, and mass gathering) considered for the simulation. This value can be imposed depending on the overall outdoor density;
- **the percentage of outdoor and indoor users**, to distinguishing the main category of position for the users. In this case, outdoor users are divided into Outdoor Only (OO), e.g. passers-by, and Prevalent outdoor (PO), such as people in dehors or other attraction poles (including green areas or porticoes). Considering building users, a part of them could be generated into special buildings, by considering their number depending on the area of the special building and its occupancy load [pp/m^2], as function of the intended use (i.e. 0.4 or 0.7pp/m^2) as in D3.2.3, Section 4.

[2] https://core.ac.uk/download/pdf/20344704.pdf (last access: 28/05/2021)

In general terms, it is considered that users can be randomly generated at a minimum distance of 0.35cm (one per patches, so as to ensure a maximum of 8 agents per square meter) which is suitable for evacuation motion purposes simulation (Almeida et al. 2012). For SLOD purposes, the random position generation is also associated to the probability of UTCI-based acceptability PA [%] for OO and PO, according to equation 2 (Cheunga and Jim 2019):

$$PA\,[\%] = \begin{cases} -0.0859\,UTCI^2 + 4.019\,UTCI + 54.119\; for\ OO\ (transient\ behaviour) \\ -0.2485\,UTCI^2 + 12.914\,UTCI - 85.681\; for\ PO\ (1 - hour\ behaviour) \end{cases} \quad \text{(Eq. 2)}$$

Transient thermal acceptability assessment is considered for OO since passersby are supposed to cross the BE(T) having a short outdoor exposure time, e.g. up to 15 minutes. 1-hour thermal acceptability assessment is introduced to not overestimate the acceptability for longer time exposure.

Users might have different ambient temperature preferences, but such differences can be more easily identified when comparing age groups. In fact, older subjects are more in favor for being surround by a warmer environment (Dong et al. 2020). Average older subjects would feel more comfortable if the temperature comfort range set-point is 2 degrees over the typical settings (T_op = 20 – 24 °C). A thermal neutral temperature for people of 60-75 and 75 – 89 years old are approximately 21.2 and 22°C, different to the established 20.4-20.5 °C (Dong et al. 2020).

However, when looking at their overall acceptability probability in the possible common temperature comfort range applied to Equation 1, these differences do not notably affect their actions for probability adaptation and PA variation in both elders and adults (Cheunga and Jim 2019), especially if considering the transient behaviour (difference of probability of about 1%). Nevertheless, elders are less capable to adapt to further thermal stress, and when they are exposed to such conditions, their morbidity and mortality rises (Kenney and Munce 2003; Bunker et al. 2016; van Hoof et al. 2017). Therefore, when analyzing the heat stress risk, it is important to consider that elderly, as youngsters and adults, would probably not be affected on the slight or moderate heat stress range condition; but elderly should be more cautious when reaching the strong heat stress status. As a consequence, in SLOD-only simulations, differences on PA will be initially overlooked but their effects on the individuals will be considered as an evaluation output.

The overall swimming-lanes ABM scheme is reported in Appendix A[3]. According to Appendix A scheme, it is considered that, in case of SLOD, the random generation of users according to the thermal acceptability assessment is performed at each simulation step (ideally 5 to 15 minutes, or even the time to cross the space at 1m/s by a OO).

In case of SLOD-to-SUOD simulation, the random generation is defined once, and then the motion equation are used to calculate the each user's position at each simulation step. Basing on previous works suggestions (Almeida et al. 2012), a cellular automata approach has been selected to define users' motion equation according to the general ABM approach, and taking into account the results from experimental-based criteria for terrorism (D1.3.3) and earthquake (D1.2.5) evacuation according to the literature. This approach adopts the fundamental diagram for pedestrian motion according to the specific terrorism and earthquake

[3] A copy of the scheme is available at https://univpm.sharepoint.com/:b:/r/sites/be.s2ecure/Documenti%20condivisi/WP4/T4.1/SLOD-to-SUOD%20sim/tentative_swim.pdf?csf=1&web=1&e=b5zMQ8

conditions, according to the Kladek-based correlation (see D1.3.3 and D1.2.5 for details), as tracked in general Equation 3:

$$Vi = \begin{cases} (Vmax - Vmin) * \left(1 - e^{-0.14*\left(\frac{1}{density} - \frac{1}{denscrit}\right)}\right) + Vmin \, for \, density < denscrit \\ \max(0, densstopregr \, * \, (density \, - \, denscrit) + \, Vmin) \, for \, density > denscrit \end{cases} \quad \text{(Eq. 2)}$$

where *denscrit* [pp/m²] is the maximum experimental density for individual's motion according to D1.3.3 and D1.2.5, and $densstopregr$ is the linear regression coefficient between *denscrit* and the density that can cause the block of people (i-.e. 6pp/m²) (van der Wal et al. 2017).

Furthermore, it is considered that:

- the individual speed depends on the density of people in their motion cone (horizontal field of view of about 200°[4]), and placed to the distance that this individual could reach at his/her current speed within a reaction time of 1s, according to equation 2. When the individual moves, he/she firstly calculates the speed by including a random error (normal distribution, standard deviation equal to *Vmin* so as to consider that people can also stop their motion at *denscrit*);
- The field of view is used also to select the cells where people can move, thus "rounding" the evacuation paths and avoiding sudden movements in direction selection according to the least effort principles (Zipf 1950; Guy et al. 2010; Sarmady et al. 2014);
- a maximum speed reduction is associated depending on the age of the individuals, depending on previous works results (Bosina and Weidmann 2017). In particular, the following reduction on maximum speeds are assumed as average value of the related age ranges: toddlers, 0.53; children, 0.87; young adults, 1; adults, 0.87; elderly, 0.67;
- the individual can move of 1 cell between the neighboring ones. Thus, each simulation step just represents a part of the movement for each second, and its time length depends on the maximum evacuation speed for the whole individual sample. In other words, he/she will be allowed to move of a distance equal to his/her desired speed divided by the maximum evacuation speed. People moving at the overall maximum evacuation speed will move at each tick, while people with lower speed will wait for some ticks depending on this division;
- when the tick allows the individual to move, the individual will try to move towards the neighboring cell in his/her field of view and direction, selecting the available (not occupied) one with the higher affordance. Anyway, if the cell will be not available, he/she will choose another cell as follows: 1) maximum $Aff_{c,t}$ considering only the cells with higher $F_{d,c,t}$ and $O_{c,t}$; 2) maximum $F_{d,c,t}$ and higher $O_{c,t}$; 3) maximum $F_{p,c,t}$ and higher $F_{d,c,t}$; 4) higher $O_{c,t}$; 5) one of the other available patches; 6) otherwise (i.e. in case of congested crowd conditions), do not move;
- in case the density is too high (>4pp/m²) or the evacuation speed reduces suddenly (more than 0.3g of acceleration between two consecutive movement ticks) or the individual is moving in a counterflow (Lakoba et al. 2005; van der Wal et al. 2017), the individual can stop his/her motion because of physical contacts and falls at the ground, depending on a probability threshold comparison by a random number. He/she will wait up to about 30s (randomly selected).

[4] https://www.epd.gov.hk/eia/register/report/eiareport/eia_2522017/EIA/html/Appendix/Appendix%2011.1.pdf (last access: 26/04/2021)

Additional rules for group motion due to shared identity between members of the same family of clan are not currently implemented in view of the difficulties in evaluating the statistical presence of such elements within the simulated population, depending on the results of D3.2.3.

For terrorist act evacuation, it is considered that people placed in outdoor areas (OO and PO) will always participate to the process, because the attack is supposed to be performed in the outdoor areas. The localization of the attack could be defined to affect $R_{c,t}$ [-] values (Compare Section 2.3.1, Eq. 1.a). People in special buildings will can participate or not to the evacuation (depending on the fact that the attack is focused on the special building), while people in other buildings are not considered in the evacuation process since they will be covered by their effects, see also behavioral analysis of D1.3.3, Section 3. People too close to the attack source will participate to the evacuation process depending on a specific self-aid and survivors' percentage value.

For the earthquake assessment process, the following simplified operational flowchart has been considered according to previous works on the possibility that people can autonomously leave debris-affected areas (including buildings) and reach a safe area in an autonomous way, that is by self-aid procedures (see https://www.mdpi.com/1660-4601/14/12/1556/htm):

1. the number of people is assessed by distinguishing those who are: inside buildings, or along the porticoes, or along the streets, or initially generated on the debris affected area (that are OO or PO) in outdoor conditions (compare to sections 3.1.2 and 3.1.3); initially placed in the free-of-debris area of the outdoor spaces of the BE(T)

2. the number of people in risky conditions is calculated. The number of people who are inside buildings or initially generated on the debris affected area in outdoor conditions is multiplied by the self-aid percentage (SAP [%], equal to: 82% getting out of the collapsed buildings by self-aid; 88% also including the support from other people from the same building) and the non-collapsed area percentage (ranging from 0%, that is complete damage, to 100% that is no damage), that represents the area that can be used by people for moving and that is not characterized by heavy damages levels[5]

3. the free-of-debris outdoor area is calculated, it can host people in emergency as a safe area

4. the number of people who can reach this free-of-debris outdoor area is calculated as the sum of people's number initially placed in the free-of-debris area of the outdoor spaces of the BE(T) and the number of people in risky conditions.

5. the density of people in this free-of-debris outdoor area is calculated as the ratio between the number of people who can reach this free-of-debris outdoor area [pp] and the free-of-debris outdoor area surface [m]. Critical conditions can be reached for density higher or equal to 3 pp/m^2, due to possible physical contacts while waiting for the rescuers' arrival.

Finally, the model essentially manages the following main uncertainties for each assessed scenario, thus requiring more than one simulation and the analysis of average simulation results (D'Orazio et al. 2014): 1) random positioning of the users in outdoor spaces at the beginning of the simulation, although PA% is considered to this end; 2) instantaneous variation of the individual speed when it is calculated; 3) possibility

[5] See also https://www.iitk.ac.in/nicee/wcee/article/10_vol10_5989.pdf (last access: 30/03/2021)

to stop the evacuation because of overcrowding/counterflows; 4) random selection of the individuals' movement order at each tick.

2.4 Output definition: basic metrics for results comparisons and BETs analysis

In this first phase of the model development, it is assumed the simulator will be used to support **stakeholders and related designer**, being a toolkit for assessing the BE(T) resilience and comparing the probable impact of solutions for risk-mitigation measures in the BE (Hissel et al. 2014; Bernardini and Ferreira 2020). Thus, simple outputs to represent the whole process are firstly considered to describe the disaster conditions in the BE(T), by mainly focusing on (Ronchi et al. 2013; van der Wal et al. 2021; Bernardini et al. 2021):

- **timing issues**, that are:
    - for SUODs, evacuation times, starting from the evacuation curve representation
    - for SLODs, exposure times, assigning the exposure time in certain conditions to each user in the open space
- **location** issues, that are the number of users for each type of area (e.g. safe areas for SUODs), and the position and number of users in critical boundary conditions (e.g. overcrowding, interactions with debris and so on), thus collecting the individuals' trajectories from a general perspective (e.g. counter of the usage of each patch in the BE by users, together with their related timing). For SUOD-earthquakes, the simplified analysis of pedestrian density in the free-of-debris-area is performed as in Section 2.3.2;
- **behavioural** issue, by counting the number of users adopting each behaviour or involved in specific actions, also in reference to their location (e.g. number of people's fall over the simulation time and their position).

3. Software implementation

Steps in the model input-output process also using Netlogo function scheme (Wilensky 1999), according to the general workflow of Figure 2:

1. defining the BET conditions in terms of SLOD, SUOD and geometrical/intended uses features, depending on the specific software to be used, so as to provide raster file, e.g. PNG or BITMAP and import it, basing on the procedures of http://ccl.northwestern.edu/netlogo/docs/dict/import-drawing.html (Section 3.1). The setup creation is performed by generating a specific NetLogo tool which exports input scenarios for further simulations by means of CSV files
2. defining the User's setup by the software interface, so as to additionally provide the possibility to perform repetitions in the analysis by means of automated script (e.g. R script for sensitive analysis) (Salecker et al. 2019) (Section 3.2). This setup and simulation running mode is performed by generating a specific NetLogo tool, that could use the outputs from the one of previous point 1
3. output analysis according to basic behavioural-based metrics (section 3.4)

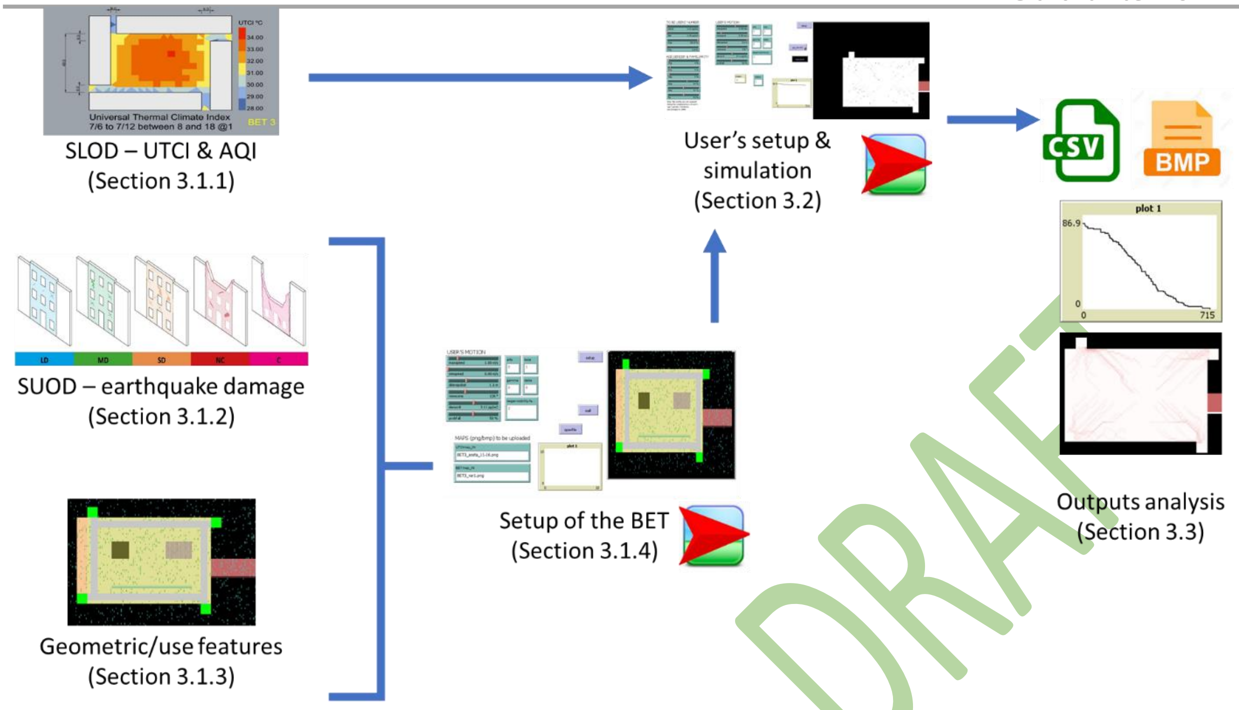

Figure 2.General workflow scheme with reference to the specific sections where concepts and functioning is explained

3.1 BET input setup for the simulator

3.1.1 SLOD input definition[6]

2 Software tools were utilized for mapping the risk of the most critical SLOD disasters. The procedure for doing so its described in the following sections, and has been summarized in Figure 3.

[6] By POLIMI collaborators

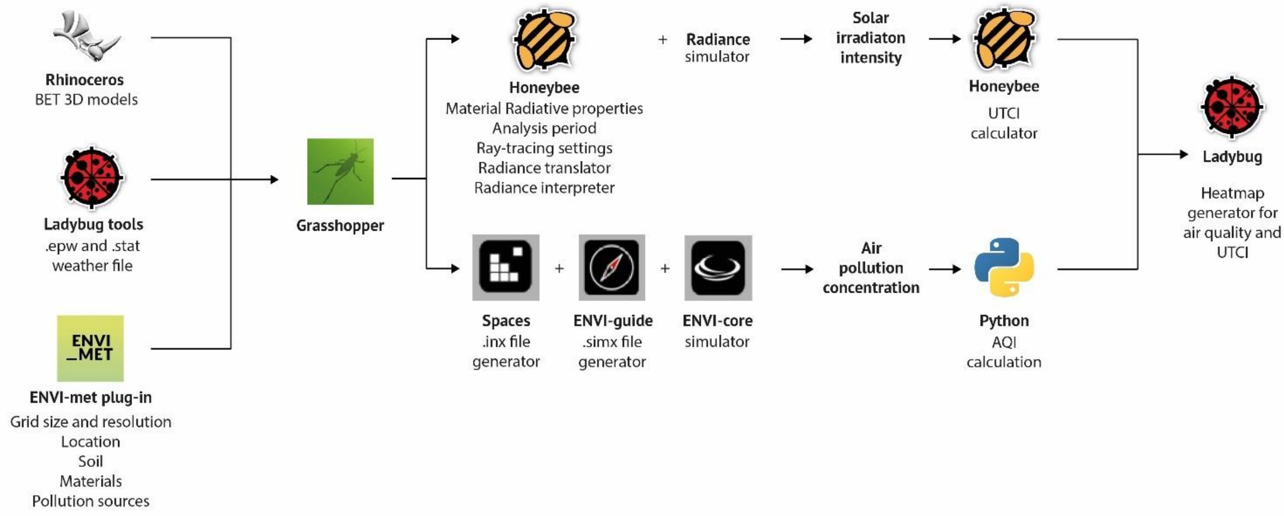

Figure 3.Software scheme for SLODs simulations

Rhinoceros + GH + Ladybug tools

GH + ladybug tools of Rhinoceros have been exploited to realize simulations for the distribution of solar radiation in different urban context, for different periods, averaging the conditions in each point of the analysis grid. Having a granular and distributed effect of heat it was possible to compute for every node of the analysis grid, the risk factor allocated for heat stress risk (I.e. UTCI); also it was possible to allocate a color to every value to visually communicate the risk condition at every point of the different urban units.

Finally, after processing and structuring data output from ENVIMET, it was possible to repeat the same steps mentioned above but for the air quality risk index selected (i.e. AQI). Then export qualitative and quantitative data for interoperability with further agent-based modelling to evaluate people behaviour.

Limitations

- Angular dependance of the radiative properties of the materials is not included;
- Wind speed spatial distribution has not been considered, instead a robust approximation was done by modifying the wind speed values to urban spaces from those contained in the weather file;
- Mean radiant temperature has been not calculated for every node, but instead it was assumed as equal to air temperature;
- Tree trunk shading potential is neglected.

ENVI-MET

Profiting from the complex models of environmental interaction integrated in ENVIMET, it was decided to use it for estimating the dynamics of air pollutants dispersion within different urban contexts. It is based on three-dimensional computational fluid dynamics (CFD) model, tailored for simulating several urban atmospheric processes. Moreover, its interoperability with Rhinoceros + GH + Ladybug tools was also an advantage.

ENVIMET allowed to estimate for every node of a user-defined analysis grid the pollutant concentrations within different contexts and at different times of the year.

Having a granular and distributed concentration of pollutants, it was possible to:

- Export such pollutant concentration values, for different positions and hours of the analysis period.

Then:

- Average for every node, the values obtained of pollutant concentration of the analysed hours.
- compute for every node of the analysis grid, the risk factor allocated for air quality risk.

Limitations

- Long machine time for every simulation;
- Low flexibility while defining the analysis grid;
- Limited pollutant absorption models for vertical greenery;
- Time-history of background pollution integration was not possible, which was simplified by adding an average value;
- Recreation of all pollutant sources was not feasible, no information was available.
- The trunk of trees is not considered in the model.

Assumptions

The geometries selected for simulations were the ones defined within D.3.2.1 as urban unit archetypes of Italian piazzas.

Simulations have been performed in different climates to analyse a wider range of cases. The most frequent climates in Italy were chosen according to the Köppen-Geiger classification: Cfa, Csa, Cfb, Dfb. Thus, four cities have been selected for simulations, and to extract weather files from, these are: Milan (Cfa), Rome (Csa), Bolzano (Cfb) and Aosta (Dfb).

Figure 4. Koppen-Geiger climate classification map for Italy (2071-2100).

For each climate it was necessary to select a suitable simulation period for both SLODs taken into consideration. To do that, the .STAT weather file and the Ladybug tools plug-in for Grasshopper were used, individuating the hottest week by climate. Given the tools limitations (ENVIMET), few hours from a week-time are valid when studying the heat island effect. However, for air pollution concentrations, a different time resolution was needed. Therefore, six hours, from 11:00 till 16:00, during the hottest day of the year was established.

It is necessary to point out that air pollution has been considered during the hottest week in order to analyze two phenomena at the same time. If the purpose of the study is to analyse only atmospheric pollution and not rising temperatures, it is strongly recommended to consider the most polluted week of the year.

The .EPW files were exploited not only for dry-bulb air temperature but also for information about: relative humidity, solar radiation, wind speed and precipitation. As regards wind data, it was necessary to establish a constant criteria to set the wind speed and direction. For this reason, the prevailing wind direction and the most recurrent speed over 0 m/s have been selected in each climate for the analysed period.

To better represent the urban pollution situation, background air pollutants concentrations are required for air pollution dispersion simulations. These concentrations have been calculated by considering five year pollution data collected from ARPA's air quality station network (Italian regional agency for environmental protection). Only data about the hottest weeks have been taken into consideration, and the median for each pollutant concentration over such week from 11.00 am till 16.00 pm was calculated.

Traffic was assumed as the only pollutant source, as including other types would require expeditive surveys. The settings used for traffic concentrations were set based on the HBEFA (Handbook Emission Factors for Rad Transport), which provides emission factors for all current vehicle categories (i.e. PC, LDV, HGV, buses, coaches and motor cycles) for a wide variety of traffic situations.

Traffic location within the BE is not random. Additional sets of simulations are generated based on the traffic position. An analysis was made from satellite images of the studied squares. For each square, the position of streets has been tracked to understand which was the most recurrent configuration. The most common types of squares are two and correspond to two opposite situations: square without traffic and square with traffic on the perimeter. Hence, the 9 BETs have been simulated in 4 different climates in 2 different traffic conditions: one without roads inside the square, the second with perimetral traffic inside the square.

3.1.2 SUOD input definition: debris due to earthquake[7]

Scenarios related to SUOD, and more specifically to earthquake, are defined by means of two different steps: the first, to assess the vulnerability of the built front facing the OS; the second, starting from the results of the vulnerability assessment, to quantify the consequent amount of debris falling from the facades following the seismic event. In greater detail, the quantity that defines the scenarios for the consequent simulation by means of Netlogo is the depth of the debris at the interface between the building and the OS in the BET.

Both the mentioned methods (vulnerability assessment and debris assessment) are innovative expeditious methods developed by the research team starting from empirical (Calvi et al. 2006; D'Ayala 2013) and analytical (Ferreira et al. 2014; Formisano et al. 2015) methods , validated by means of (i) comparison with similar expeditious method in literature and (ii) against real data from the 2016 seismic even in Central Italy. Both the methods (for vulnerability and for debris) contribute to literature in that they are able to provide reliable quantitative information based on rapid external surveys of the façades. Additional details with respect to the base information gathered from the façade (such as the presence of ring beams or the exact type of material constituting the masonry) can be included to further add precision to the assessment.

Details on the two expeditious methods are available in the article (Bernabei et al. 2021b) and in an undergoing paper by the same authors. Below, we provide a brief explanation of the two methods.

[7] By UNIPG collaborators

Vulnerability Assessment

Vulnerability is evaluated in an expeditious manner, based on a new empirical method presented in (Bernabei et al. 2021b) and validated against existing empirical and analytical methods, as well as real case studies. The assessment is based on 5 parameters related to both geometry and construction features of the façade of the investigated building composing the built front on the OS. The innovativeness of the method is to being able to provide reliable information about the vulnerability buildings' facades by means of external surveys and images. The parameters are floor numbers, specific weight of the masonry, slenderness of the façade, roof type and amount of openings. For each parameter, four classes of increasing vulnerability are assigned, and multiplied by the weight of each parameter. Based on these computations, the vulnerability (I_{vf}) of the façade is defined; it is then combined with the hazard level by means of the damage matrix (Figure 5, elaborated from (Bernabei et al. 2021a)). The output of the matrix are the damage states of the façade, which are thus defined as light-, medium- and severe- damage, near collapse (collapse of up to 25% of the façade) and collapse of the façade (more of the 75% of the façade) (Figure 6). Only the last two cases produce debris, which leads to the following section.

The above described damage scale (specifically referred to façade) is then correlated to the EMS-98 scale (referred to the entire building) for determining the percentage of people that are able to evacuate according to section 2.3.2. The five damage states correlations are as follows: ND=D0, LD=D1, MD=D2, SD=D3, NC=D4, C=D5.

Regarding the correlation of the two scales with respect to the maximum damage (C-D5), it is possible that C state (damage scale for façade) cause the only collapse of the façade but not of the entire building, as by D5 (EMS-98 scale). However, we selected C=D5 in a precautionary manner.

Severity of damage grade →

		VULNERABILITY - I_{vf}		
		LOW *(≤ 54)*	MEDIUM *(55 - 69)*	HIGH *(≥ 70)*
HAZARD - RP	975	SD NC	NC C	C
	475	MD SD	SD NC	NC C
	101	LD MD	MD SD	SD NC

Figure 5. Damage matrix: vulnerability ranges and return period determine damage state: light- (LD), medium- (MD) and severe-damage (SD), near collapse (NC) and collapse (C) of the façade.

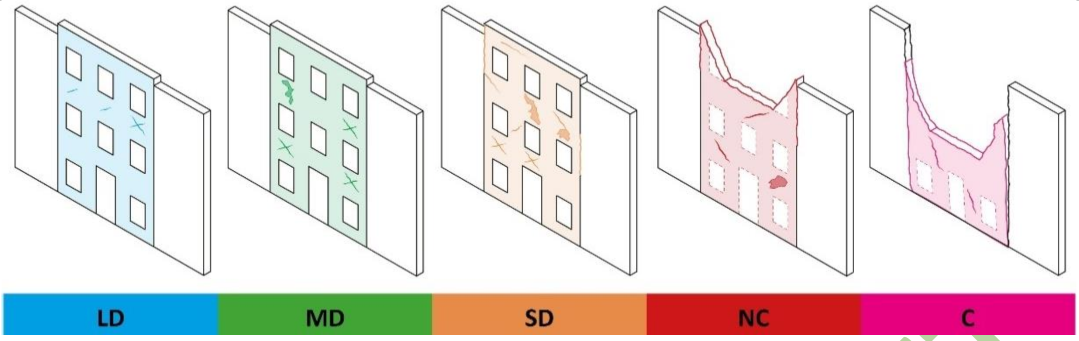

Figure 6. Damage states of the facades.

Given that the BET are typologies of built environment (D3.1.1 and D3.1.2), and thus general types, the evaluation of the vulnerability is based on four levels of increasing vulnerability (lv_1-lv_4) to represent many possible scenarios. Each level of vulnerability for the BETs is defined starting from the classes of the parameters, as illustrated in Figure 7, while the height of the buildings (P1) varies according to the specific BET (as from D3.2.1).

	Parameters P_i	Class c_i				Weight W_i
P1	Floors number	*1 floor*	*2 floors*	*3 floors*	*4 or more floors*	30.74
		0.18	0.35	0.51	1	
P2	Specific weight [kN/m³]	*greater than 23*	*from 20 to 22*	*from 17 to 19*	*from 11 to 16*	6.56
		0.71	0.77	0.83	1	
P3	Slenderness	*less than 9*	*from 10 to 12*	*from 13 to 17*	*greater than 18*	25.41
		0.19	0.32	0.51	1	
P4	Roof type	*flat roof*	*non-pushing roof*	*slightly-pushing roof*	*pushing roof*	23.77
		0	0.21	0.41	1	
P5	Openings	*less than 4%*	*from 5% to 10%*	*from 11% to 18%*	*greater than 18%*	13.52
		0.54	0.77	0.88	1	
		lv1	lv2	lv3	lv4	

lv1= (c2xw2)+(c3xw3)+(c4xw4)=(0.71x6.56)+(0.19x25.41)+(0x23.77)+(0.54x13.52)=19.80

Figure 7. Definition of the vulnerability levels for the BETs.

The four lvs, are then combined with the three levels of hazard (return period (RP) equal to 975, 475, 101) to obtain the damage state, as by Figure 5. Only NC and C are considered for debris calculations.

Debris Assessment

The calculation of the debris is evaluated by means of an experimental expeditious method, actually the subject of an ongoing paper. The debris width is calculated as follows:

$$w_D = \sqrt{V_D \Big/ \left(\frac{\tan\beta}{2\,n \cdot m}\right)} \qquad \text{Eq. 1}$$

Where:
Wd is debris width;

Vd is the volume of the overturning portion of the façade, obtained by multiplying the height of the overturning façade for the width of the overturning masonry portion (for a unity of a linear meter), for a coefficient of 1.3 considering the amplification of volume given by the demolition material;
β is the friction angle of the masonry, corresponding to 30° (mean value of sand and gravel);
n and ***m*** are reduction coefficients: n is the number of overturning floors (height of the portion of overturning façade) and m is related to the specific weight of the masonry types, fixed at 1.25.

For further detailing ***n*** for the BETs, it depends on the damage state:

- For **NC case**,
  n=1 floor=3.4 m in the case of 2 or 3 floors buildings;
  n=2 floors=6.8 m in the case of 4 or more floors for standard buildings, while n=2 floors=8 m in the case of 4 or more floors for palaces/special buildings;
- For **C case**, n=height of the building

Assumptions
The methods assume that the buildings are all masonry buildings, as common in historical centers. For the BETs, an average height of each floor has been defined as 3.4 m, and the thickness of the walls 0.5 m, based on observations of the sample buildings.

Limitations
The vulnerability method has been found to overestimate vulnerability in the case of anti-seismic devices: indeed, inter-story ring beam and the effectiveness of tie rods are a source of uncertainties, as they are not always detectable by an external survey. Moreover, the vulnerability and debris method is valid for masonry buildings, which still are the most common typology in historical centers.

3.1.3 SLOD+SUOD implementation in the Netlogo process

The BET input setup is provided according to 1 to 3 different raster images. These files should be saved as a PNG or BITMAP file and placed in the same folder of the simulator (as a *.nlogo file). They should represent the BET with a 300DPI resolution (encourage, at least 72DPI), and with a scale 1 pixel equal to 0.35m (at least, 1 pixel per meter). In the Netlogo code, the resize-world command is used to define the effective dimension of the space as a multiple of the 0.35m grid.

Figure 8 shows an example of the BET geometry and its spaces (i.e. an example relating to BET 3 with a special building). Each color refers to a different intended use. In particular, buildings are black, special buildings are red, dehors are light brown, green areas are dark green, general areas for OO (e.g. sidewalks) are in yellow, streets (vehicle areas inside the BE(T)) are in grey, porticoes are in pink, monuments and other not accessible areas are in dark brown. Finally, the access streets are in light green. These access streets can be used in earthquake simulation to generate eventual users from interfering SoR (through a constant flow of 1.5pp/s), and in terrorist act simulation as exits/safe areas for the evacuation process.

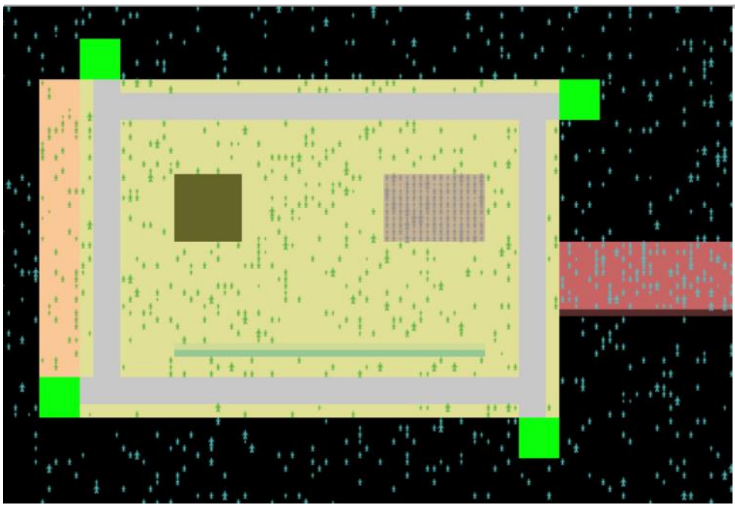

Figure 8. BET representation example: geometry and BET spaces input raster image

Figure 9 shows the SLOD input data for the user' acceptability assessment in HRM conditions, according to the UTCI scale results[8] calculated via the process in Section 3.1.1. Finally, Figure 10 shows the overlapping of the debris area (in red: 187,0,0) due to earthquake occurrence according to Section 3.1.2 and an example of BET 3 geometry derived from Table 2 criteria. The depth of the debris area is considered as uniform because of the uniform building heights along the different BET sides.

[8] compare D2.2.1 and to http://www.utci.org/utci_poster.pdf (last access: 25.06.2021)

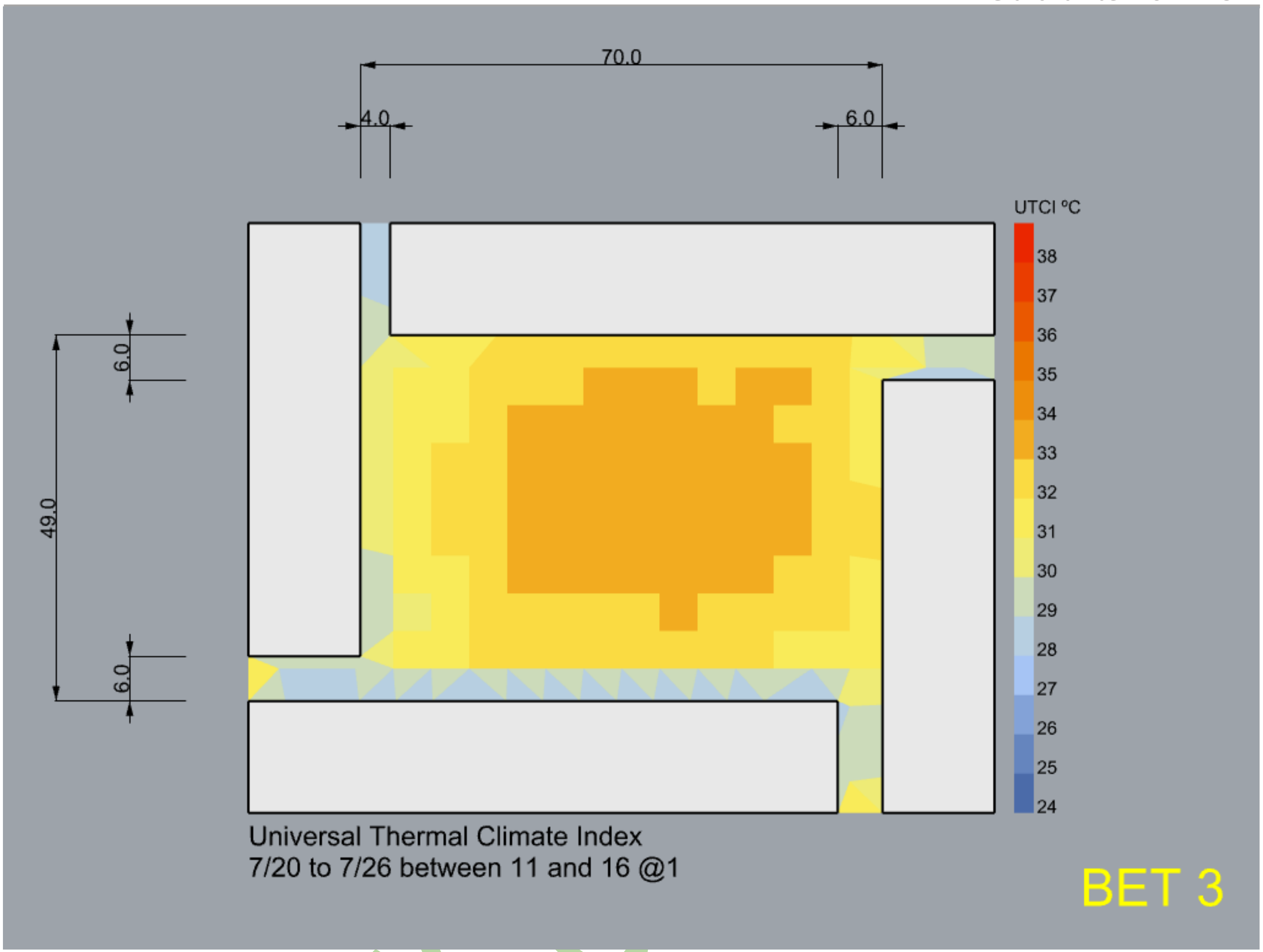

Figure 9. example of SLOD conditions based on HRM input raster image, referring to BET 3 for the Aosta -related scenario. This image also reports the UTCI scale on the right to associate the values on the cells, and the dimension of the BET.

*Table 2. RGB for geometry/use and UTCI values: conversion table. *: RGB values out of the scale should be extended according to specific scenarios*

Geometry/use (Figure 8)	**RGB**	**UTCI value (Figure 9) °C**	**RGB***
BUILDINGS	0 0 0	24	75;107;169
SPECIAL buildings	200 100 100	25	101;133;190
GREEN AREA	150 200 150	26	131;162;215
DEHORS	200 180 150	27	166;196;244
PORTICOES	250 200 150	28	183;207;225
PEDESTRIAN area (for OO)	225 225 150	29	204;219;186
VEHICULAR areas	200 200 200	30	238;235;118
WATER	40 100 200	31	249;235;89
PERMANENT OBSTACLES	70 60 50		
ACCESS STREETS (used as safe areas in terrorist act evacuation)	10 255 10	32	250;219;66
TEMPORARY / LOW OBSTACLES (foldable)	140 100 60	33	242;172;32

Other risk maps		34	237;142;12
DEBRIS AREA	189 0 0	35	234;119;0
ATTACK AREAS	200 100 0	36	234;88;0

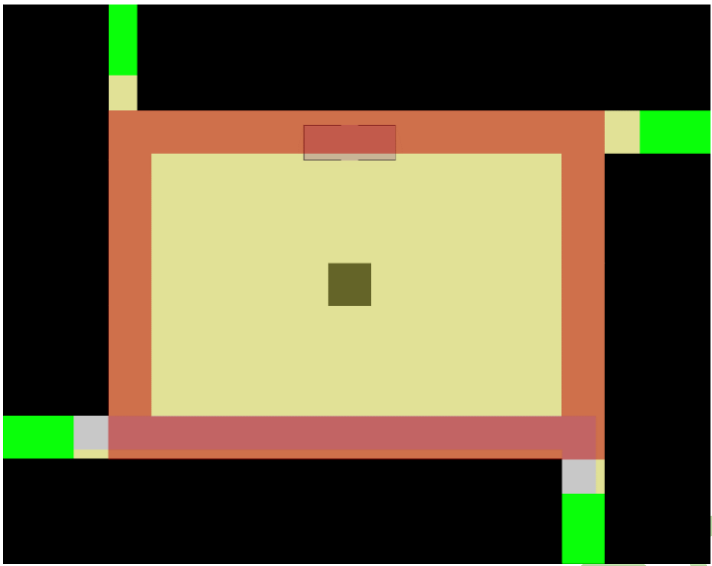

Figure 10. SUOD conditions based on SRM input raster image (red area) overlapped to a BET geometry elaborated according to Figure 8 example.

Figure 11 shows the Netlogo Interface describing the main input parameters for the setup of the BET, that comprises the scenario description (BETmap_IN) and the UTCI data upload according to Section 3.1.1 simulation (UTCImap_IN), on the left, the input patches parameters for Standard Priority Queue Flood Fill Algorithm - PQFFA (including the overall grid dimension, including buildings) and the affordance-based assessment of open space, so as to provide the input data for the simulation tool as described in Section 3.2.

In particular, the number of cells in the two direction (xcell, ycell) should be calculated according to the original dimension of the bmp/png depending on the BET, e.g.: BET image to be uploaded: 3172 * 3172 pixel => 100m * 79m => for patchsize-m=0.35, xcell x ycell = 286 x 286. Anyway, take care while simulating (view update in continuous mode) to evaluate how many blue, white or red patches are present in the graphical interface on the right. You can change xcell,ycell to reduce as possible the number of these patches (see the "correct the patches sector value in case there are patches with colors that are different from those of the color assignement process" commands). Similarly, the patchsize-m [m] provides the dimension of the patch in meters: the suggested value is 0.35, equal to the shoulder dimension of the individual, thus assuming a possible maximum density of 6 to 7 users per square meter in simulation according to the Cellular Automata approach. This value must correspond to xcell-ycell combination.

In particular, this application provides, in output:

- The results of the PQFFA only basing on the distance to a safe area, by considering "entering" or "leaving" conditions, to derive $F_{d,c,t}$, respectively in earthquake and terrorist acts simulations
- The results of the distance from obstacles, to be included in the affordance-based guidance of people (to derive $O_{c,t}$
- The results of the risk for the patches in the scenario depending on the attack map input, to derive $R_{c,t}$ in static conditions (e.g. in case of a bomb). In such case, the source of the attack given by the input attack map is used to also detect obstacles which can be used as temporary safe areas because they are not visible from the source of the attack

The viewmaps of the data are also provided in *.bmp format, as in the example of Figure 12, where smaller distance (Fdt tends to 1) to the safe areas is shown in black, as well as the buildings, while greater distance is shown in white (Fdt tends to 0).

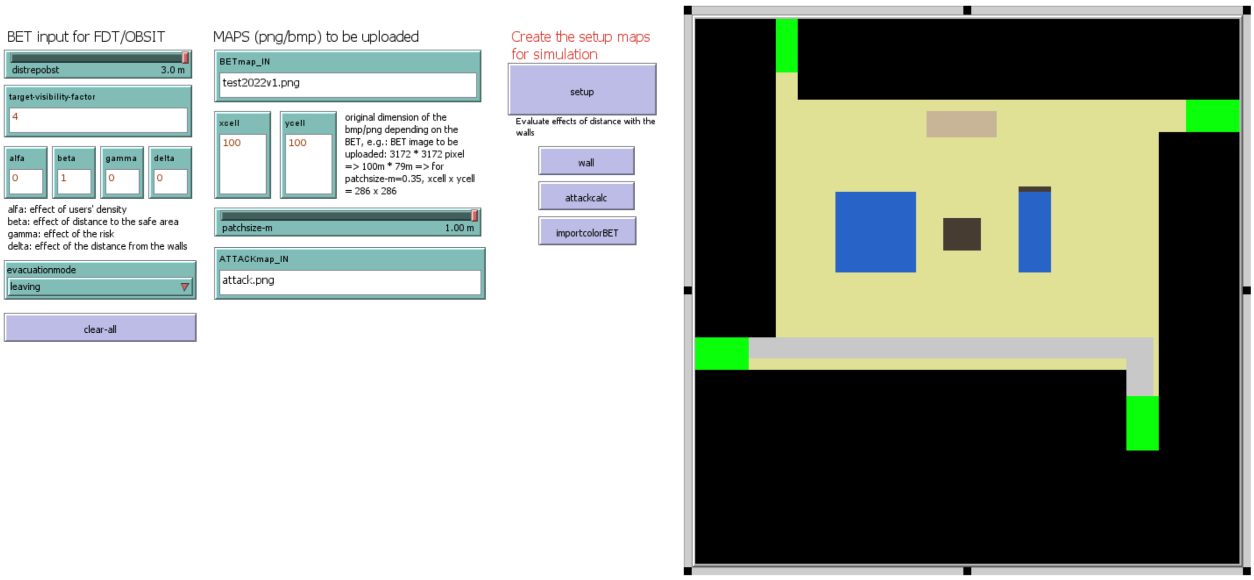

Figure 11. Input model parameters in Netlogo according to the general rules for users' typology

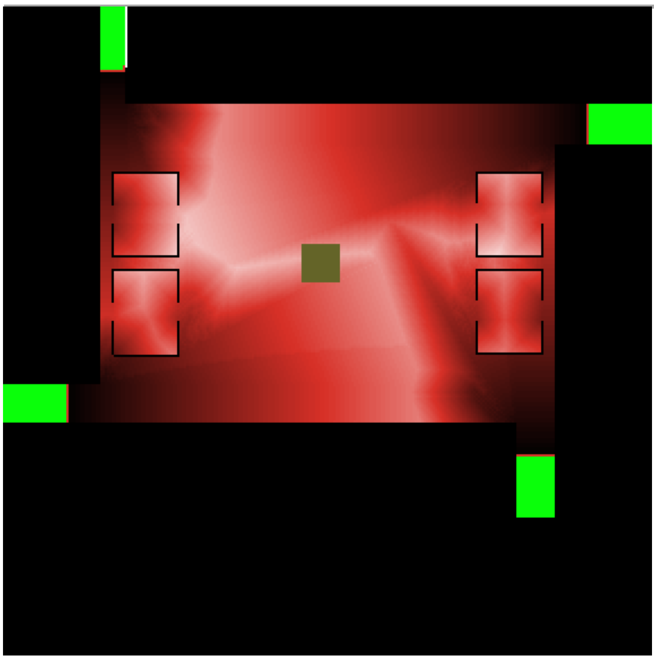

Figure 12. Fdt.bmp file as an output of the input model in Netlogo*

3.2 Users' setup for the simulator and interface description

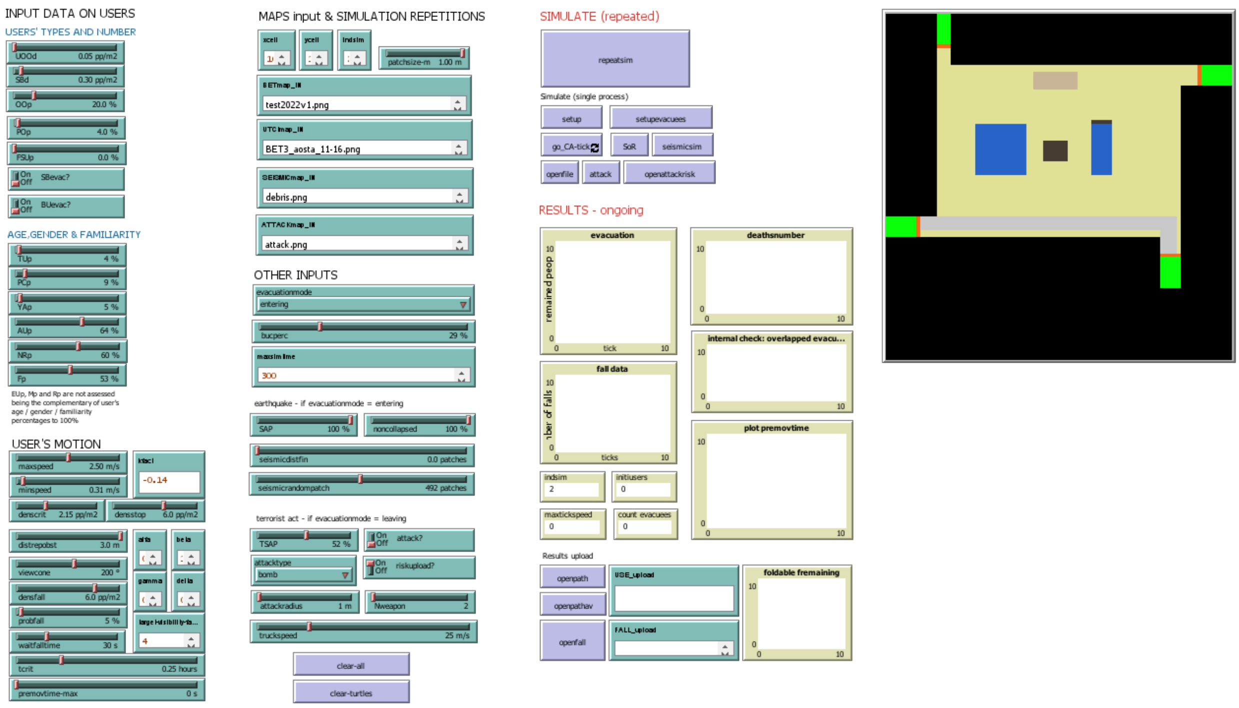

Figure 13 shows the interface for the users' setup and simulation tool, which uses input data from the setup of the BET, the UTCI input files and the statistics to generate the number and types of people to be involved in the scenario.

The left part of the panel shows the data on the users' characterization in terms of age and types. UOO refers to users' overall outdoor value, SB refers to the special buildings. *d* subscript refers to density, while *p* to percentage values. In particular, UOOd directly comes from the D3.2.3 – Section 6.1 results and could be the one referring to the whole conditions (the median value, which relies on the whole sample of assessed BEs) or to specific conditions for some BET or for the specific day/time in which the BET is analysed (i.e. depending on D3.2.3 – Section 5 UOOd over day time diagrams for working days).

The central part of the panel (Users' motion) refers to the variables about users' movement, so as to delineate the fundamental diagram of pedestrian's dynamic, the view cone, the critical density and so the probability to fall in case of high density or counterflowing. The weights for path choices are also included, as well as the critical exposure time *tcrit* (hours) for heatwave exposure, according to D4.2.3, Section 2.1, which is calculated within this application.

In the bottom central part, there are the maps inputs in terms of overall patches dimension, and the input files to be uploaded for the scenario description (BETmap_IN) and the UTCI data upload according to Section 3.1.1 simulation (UTCImap_IN). It also includes the map on the earthquake-induced debris on the ground (red: RGB [179 0 0]). The patchsize and the xcell-ycell dimensions should be collected from the same values of the simulation setup creation. An image (png) with the attack source position (static position) could be used (ATTACKmap_IN) to alter the risk conditions (Eq. 1a) of the outdoor patches (RGB [200 100 0]).

Finally, the right part includes the simulation starting for repeated entries (repeatsim) and for single process, and, in the bottom part, the results ongoing about the evacuation curve and the graphical interface of motion, where to see the progress of users' motion during the simulation. The results upload part allows uploading and visualizing the simulation results on paths use and falls.

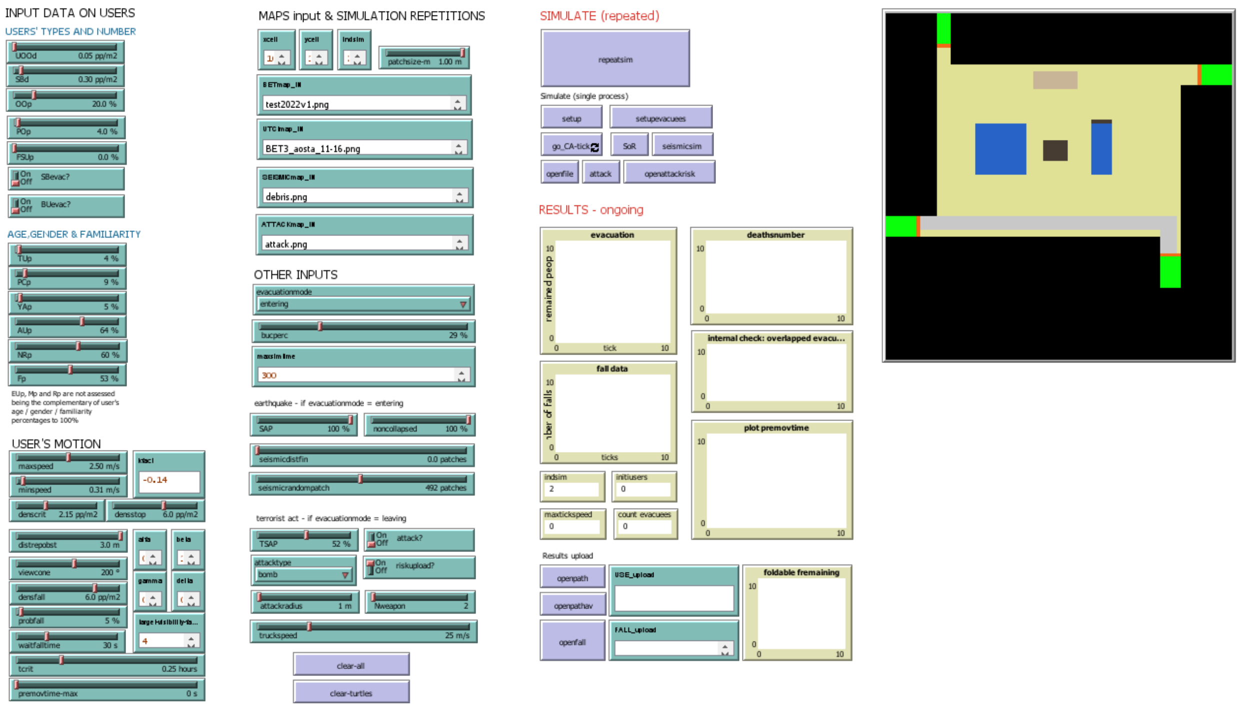

Figure 13. Input model parameters in Netlogo according to the general rules for users' typology

3.3 Output analysis: basic behavioral-based metrics

The model described in Section 3.2 provides the following output files, according to the rationale of Section 2.4, for each of the simulation repetitions which number is given by *indsim*:

- The initial position of the turtles (namely, an "turtles_started*.csv" file), in the form: *list who xcor ycor fam-type gender-type age-type position-type*
- The data on the arrival of the turtles (namely, an "turtles_arrived*.csv" file), in the form: *list indsim who xcor ycor (ticks / maxtickspeed * 0.35) fallcounter*
- The data on the space use by the turtles, referring to the patches (namely, an "space_use*.csv" file), in the form: *list indsim pxcor pycor path*
- The data on the space fall by the turltes, referring to the patches, that express how many users were blocked because of counterflows/critical density reached for each of the patch (namely, an "space_fall*.csv" file), in the form: *list indsim pxcor pycor fallnumber*
- The png data on the space_use and space_fall for each of the simulation
- The data on the water loss calculation and seismic simulation (namely, an "WLbetOO*.csv" file), only one time, since it does not depends on the turtles generation process, and in the combined form:
  - WATER LOSS DATA PER UTCI AREA: *evaluateUTCI sweatrate (count patches with [sector < 3 and sector > -1 and UTCI = evaluateUTCI]) (transient evaluateUTCI) (sweatrate * count patches with [sector < 3 and sector > -1 and UTCI = evaluateUTCI] * ((transient evaluateUTCI) / 100)*
  - WATER LOSS DATA FOR THE WHOLE BET: *(WLnum / totalareaforusers) (tcrit * WLnum / totalareaforusers)*

- The data on the seismic simulation (namely, an "WLbetOO*.csv" file), depending on the specific turltes generation conditions, since it depends on this value, and in the form: *indsim SAP noncollapsed (count turtles) safeturtles riskyturtles outarea area_nodebris SA_dens.*
- The statistics summary of the input data from the evacuation process (terrorist act) simulation (namely, an "statsummary_start_evac*.csv.csv" file), in the form*: initiusers SB OO PO BU killedbyattack notevacuating alfa beta gamma delta SBevac? BUevac? attack? attackradius SAP TSAP noncollapsed maxspeed minspeed denscrit densstop distrepobst densfall probfall waitfalltime tcrit premovtime-max BETmap_IN UTCImap_IN SEISMICmap_IN ATTACKmap_IN indsim*

In addition, the space_use and space_fall data are also reported in an overall way for all the repetitions, respectively in the form: *list pxcor pycor ((pathusetot / indsimtot) / maxuse)* and *list pxcor pycor ((falltot / indsimtot) / maxfall)*. This allows to trace the most (maximum value equal to 1) and the less (equal to 0) used/critical-for-fall patches by considering the performed *indsim* simulations having the randomness described in Section 2.3. Similarly, aggregated use and fall maps are provided also in an averaged manner (data on the path use/fall normalized from 1 (max value) to 0 (min value, not used or not falls) and with average values for neighboring patches for "void" (not used) patches).

4. Results: showing the process on BET 3

4.1 SLOD input definition[9]

For every representative city (and climate) the hottest week and day was determined, to narrow down the analysis period of the analysis (resulting in lower machine time per simulation). Based on the .STAT files, the hottest week was extracted (unless, only air pollution is studied, then the most polluted week is used); then, with the dry-bulb air temperature and total solar radiation for such week, the hottest day was individuated as well. A summary of such periods is presented in Table 3.

Table 3 - SLOD analysis periods

City / Climate	Hottest week	Hottest day
Milan (Cfa)	6th – 12th July	11th July
Rome (Csa)	10th – 16th August	15th August
Bolzano (Cfb)	29th June – 5th July	1st July
Aosta (Dfb)	20th - 26th July	25th July

Even though climate files used for simulations provide wind data, these have been considered differently. A constant criteria to set wind speed and direction was needed in order to have comparable results and understand pollutants dispersion within the BE. Thus, the prevailing wind direction and intensity have been selected.

Table 4 - Prevailing wind directions and intensities

City / Climate	Prevailing wind direction azimuth	Intensity
Milan (Cfa)	310°	1.9 m/s

[9] By POLIMI collaborators

Rome (Csa)	200°	6.0 m/s
Bolzano (Cfb)	90°	1.2 m/s
Aosta (Dfb)	90°	6.2 m/s

Materials were set based on common construction materials, the radiative properties of such materials can be found in Table 5.

Table 5 - Albedo coefficient for the selected materials

Material	Albedo
Roof	0.7
Façade	0.5
Asphalt	0.08

Only for Bet n.5 there is the possibility to integrate green areas in the modelled geometry. For this purpose, it was fundamental to determine the type of grass and trees to add in the model. In particular, the values that characterize greenery are foliage shortwave albedo and shortwave transmittance.

Table 6 - Foliage properties

Greenery	Albedo	Shortwave transmittance
Grass	0.2	0.3
Trees	0.18	0.3

As explained in §3.1.1, background air pollutants concentrations are essential to better represent the urban pollution. Analyzing ARPA data of the last five years the average pollutants background concentrations have been calculated for each city.

Table 7 - Background concentrations for each city in the analyzed period

City / Climate	NO_2 [μg/m³]	O_3 [μg/m³]	PM10 [μg/m³]	PM2.5 [μg/m³]
Milan (Cfa)	15	83	20	15
Rome (Csa)	17	61	23	12
Bolzano (Cfb)	31	31	17	12
Aosta (Dfb)	19	109	15	7

Simulations outputs

All the BETs were simulated based on the settings described so far. Results are presented both as qualitative (heatmaps) and quantitative data (values collection).

For pollution the AQI is used. Normally AQI considers all of the main threatening air pollutants. Nevertheless, PM does not vary significantly in small areas, such as those of the BETs. Also, since traffic is the only source of pollution in the modelled area, it must be considered that it is mostly responsible for NO_x production rather than PM. For this reason, the Bitmap produced for air pollution simulations are based on an AQI which only considers the distribution of NO_2 (the only pollutant within the table of suggested concentrations of air quality guidelines. (FONTE DA INSERIRE US EPA: Technical Assistance Document for the Reporting of Daily Air Quality – the Air Quality Index (AQI). (2018)

For heat stress risk, UTCI is utilized. No detail calculation on mean radiant temperature is performed, and neither detailed information on the wind speed distribution within the context was done. In fact, mean radiant temperature was considered equal to air temperature and wind direction and speed were considered to be equal to the ones provided on the weather data (.EPW file).

Then, for every node of the grid of analysis, the UTCI and the air pollutant concentrations are gathered and averaged for every node in the whole of the analysis period:

- For heat stress, from 11:00 till 16:00 for the hottest week (6 values per day per node);
- For air pollution, from 11:00 till 16:00 for the hottest day (6 values per node).

Then, AQI is computed for every node, and both UTCI and AQI are rounded to its integer to simplify and ease the interoperability with the occupant behavior tool. Finally, two heatmaps are generated, to every cell of the analysis grid a color is allocated based on the AQI and UTCI computed. The colormap used for AQ follows the guidelines made by EPA (FONTE DI PRIMA), while heat stress related risk is presented from blue to red from a set of colors from Ladybug tool default.

Qualitative output example for BET 3

An example of the bitmap realised for each simulation is provided in Table 8 and Table 9. In detail, these tables present results for the BET n.3, simulated in the four different climates, with different traffic conditions.

Table 8 - AQI outputs for the BET3, simulated in different climates and with different traffic conditions.

AQI	
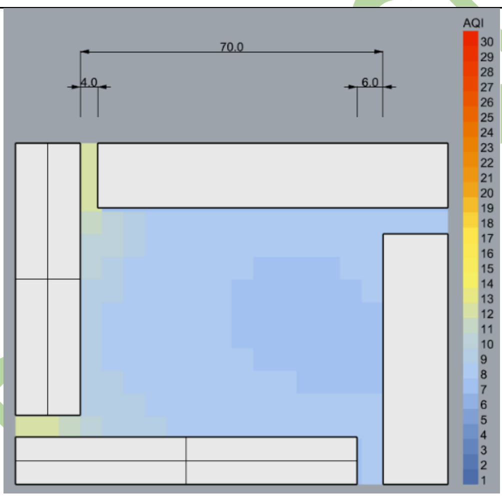 AQI for BET 3 – Milan, no traffic	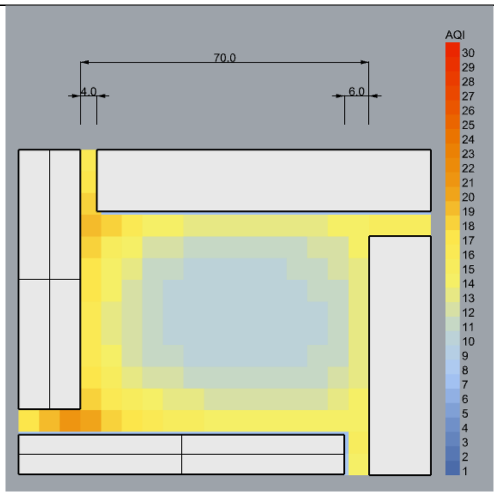 AQI for BET 3 – Milan, with traffic

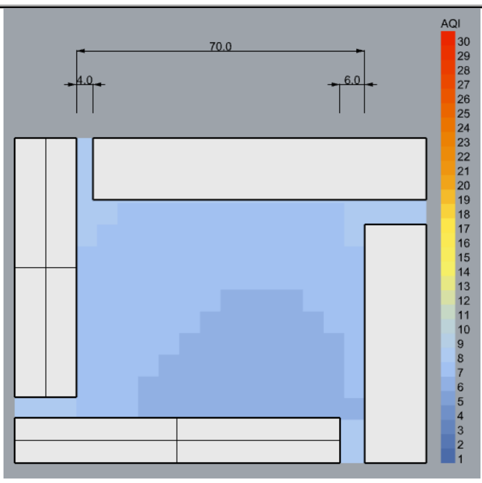

AQI for BET 3 – Rome, no traffic

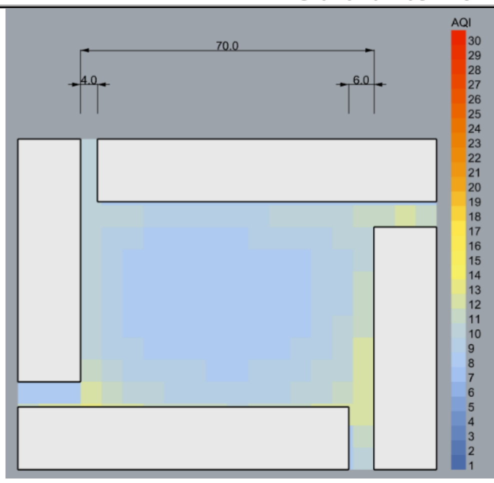

AQI for BET 3 – Rome, with traffic

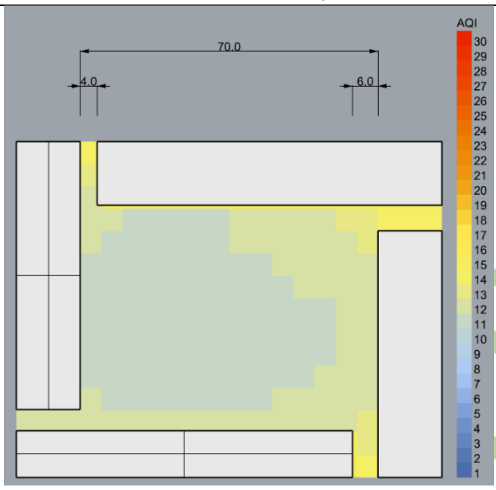

AQI for BET 3 – Bolzano, no traffic

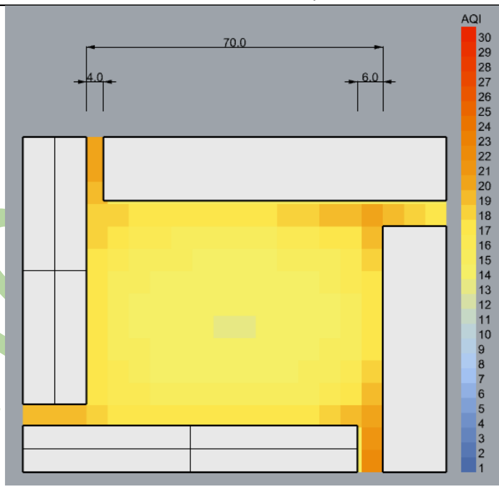

AQI for BET 3 – Bolzano, with traffic

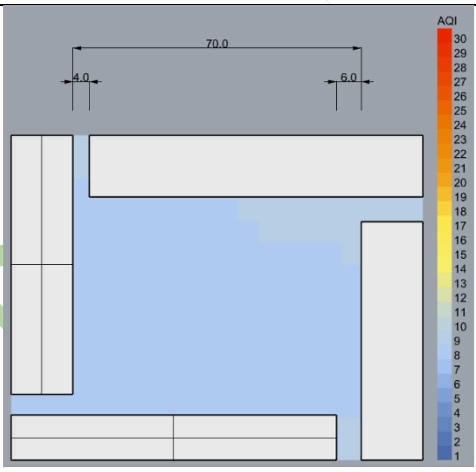

AQI for BET 3 – Aosta, no traffic

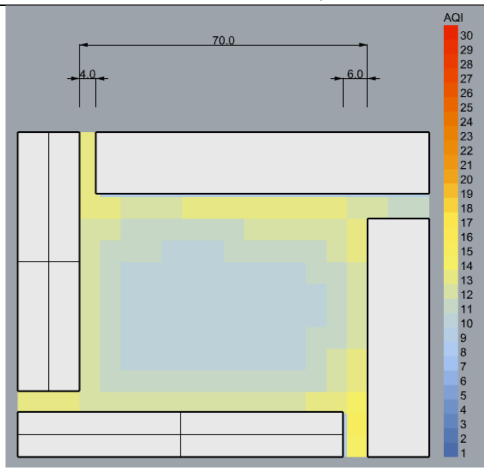

AQI for BET 3 – Aosta, with traffic

Table 9 - UTCI outputs for the BET3, simulated in different climates.

UTCI

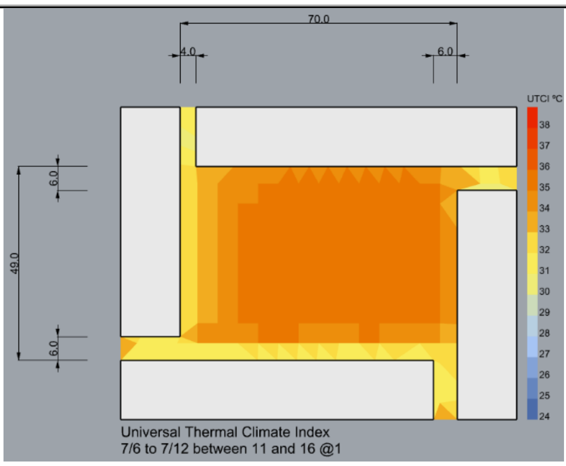

UTCI for BET 3 - Milan

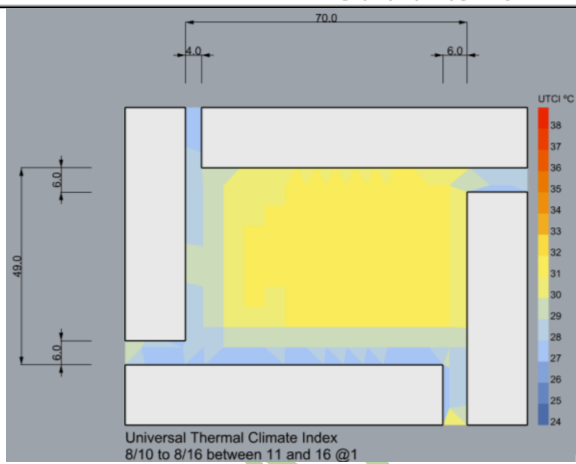

UTCI for BET 3 – Rome

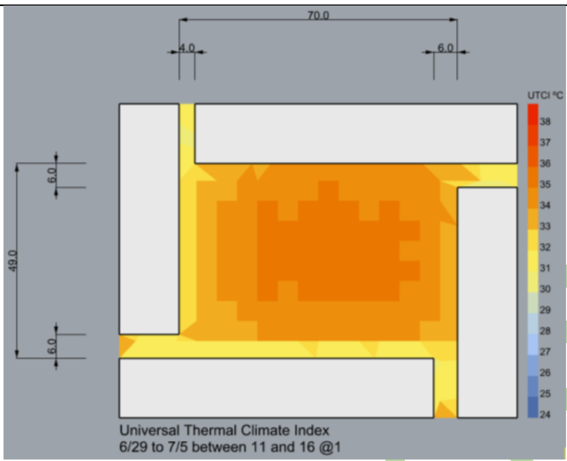

UTCI for BET 3 - Bolzano

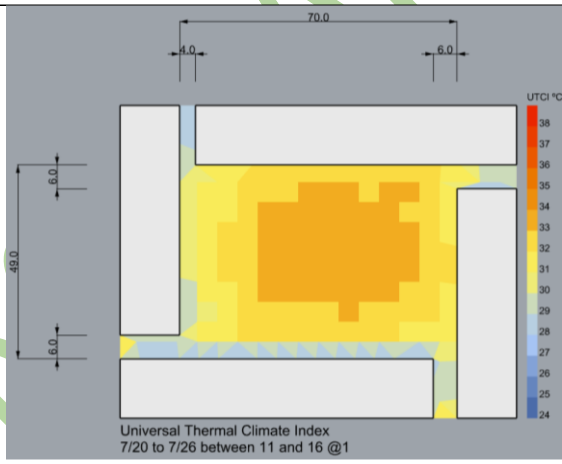

UTCI for BET 3 - Aosta

4.2 SUOD results for BET3: earthquake damage assessment[10]

For every BET, the levels of vulnerability (Ivs) are defined, as illustrated in section 3.1.2, Figure 7. Thus, the input data for each BET is only the average height (H_{av}) of the buildings of the CBF in the BET. Then, for each Ivs, the damage matrix is interrogated (Figure 5): if the resulting Iv gives a damage state corresponding to NC or C, then the debris is calculated with the formula in Eq.1.

As an exemplificative case, BET3 resulting output is illustrated in Figure 14.

[10] By UNIPG collaborators

BET 3										
H_{av} = 15 m	Iv_2 = 62	475	WD [m]	Iv_3 = 73	475	WD [m]	Iv_4 = 100	475	WD [m]
		SD	0		NC	6.19		NC	6.19
		975	WD [m]		975	WD [m]		975	WD [m]
		NC	6.19		C	13		C	13

Figure 14. Input and output values for BET3.

These numerical values can be graphically elaborated (Figure 15 and Figure 16), and the delivered information is bi-dimensional (debris depth). All the needed information for the following simulation are retrievable from the bi-dimensional debris width, however, as the angle β (from the formula in Eq. 1) is given and equal to 30°, it is then possible to evaluate the height of the debris on the façade and to obtain a tri-dimensional file (Figure 17).

Appendix B reports the whole damage conditions for all the BETs according to the proposed approach. See D3.2.1 for the BET geometry definition.

BET 3 Hav=15 m	MEDIUM VULNERABILITY Iv2= 62	HIGH VULNERABILITY Iv3=73 and Iv4=100
RP= 975	w_d=6.19 m 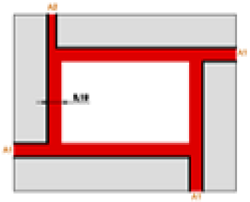	w_d=13 m 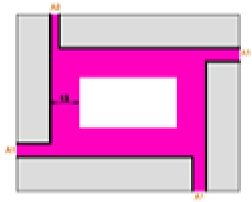
RP = 475	w_d=0 m 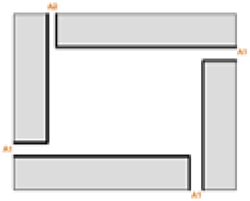	w_d=6.19 m 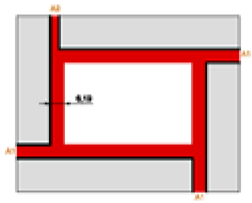

Figure 15. Output results for debris depth of BET3.

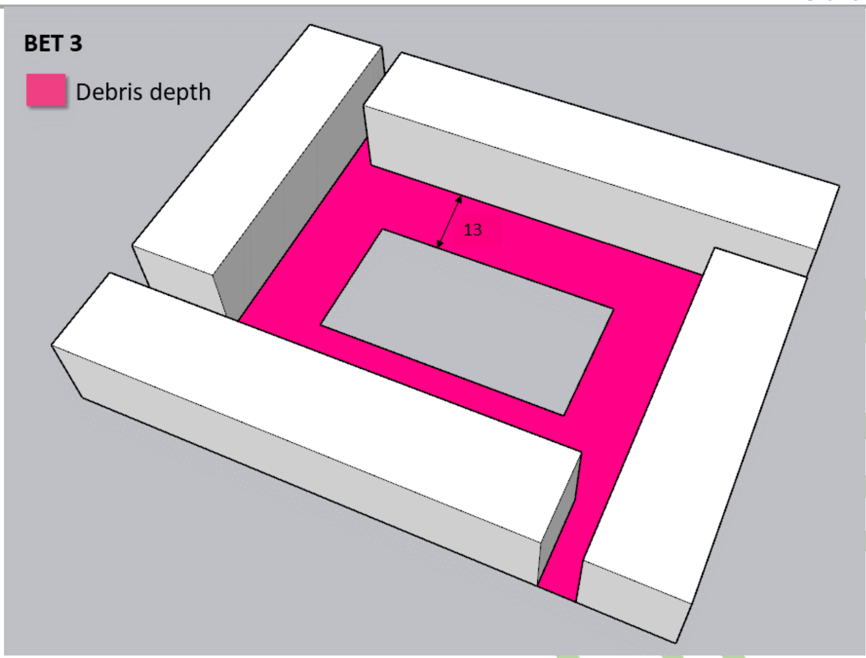

Figure 16. 3d visualization of bi-dimensional debris depth information in BET3 for C case.

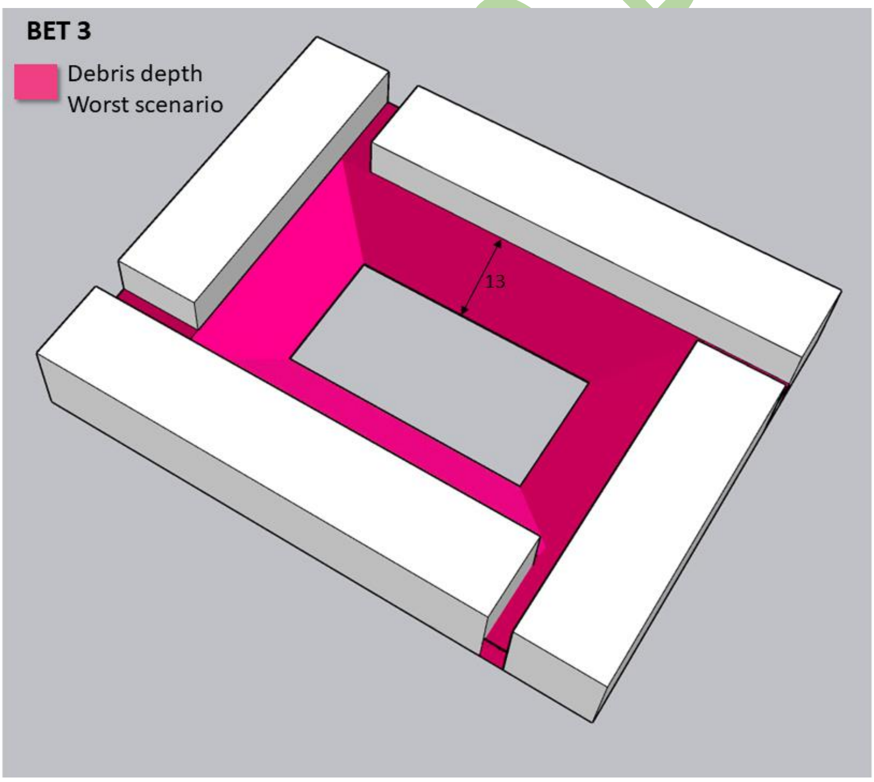

Figure 17. 3d visualization of tri-dimensional debris volume information in BET3 for C case.

4.3 SLOD+SUOD simulations

This section resumes the simulation results for the BET3 condition by assuming the Aosta UTCI conditions and the C case conditions for seismic risk (SAP=88%, non collapsed area=100%), plus the presence of a risk source for terrorist act in the outdoor area in the top-right corner of the scenario. It also includes 4 areas for dehors on the left and right parts of the BET (east and west direction). In this sense, Figure 18 resumes the distance and interactions with obstacles map, thus graphically showing $P_{i,c,t}$ [-] and $F_{d,c,t}$ [-] data from a qualitative standpoint (target-visibility-factor = 4 and distrepobst = 3m).

Since all the simulations refers to the Aosta case study, the same results on water loss can be obtained. According to D4.2.3, section 2, a water loss of about 166 g/h is obtained, that imply a water loss of about 42g for 15 minutes of critical exposure.

Figure 19 resumes the evacuation data considering the case of terrorist act (people leaving the BET), according to the studied 4 conditions, while Figure 20 shows the outdoor spaces use. Finally, Table 10 collects data on terrorist acts and earthquake evacuation. In general terms, including $\mathrm{P}_{\mathrm{i,c,t}}$ and $\mathrm{OR}_{\mathrm{c,t}}$ in the local motion direction seems to limitedly alter the evacuation time for low pedestrians' density, while the number of users to be evacuated significantly increase the evacuation time, as expected. Considering the given layout, the model seems to represent the quick abandon of the center of the square, with people looking for repair towards the borders of the square itself, as noticed in real world evacuation for terrorist acts.

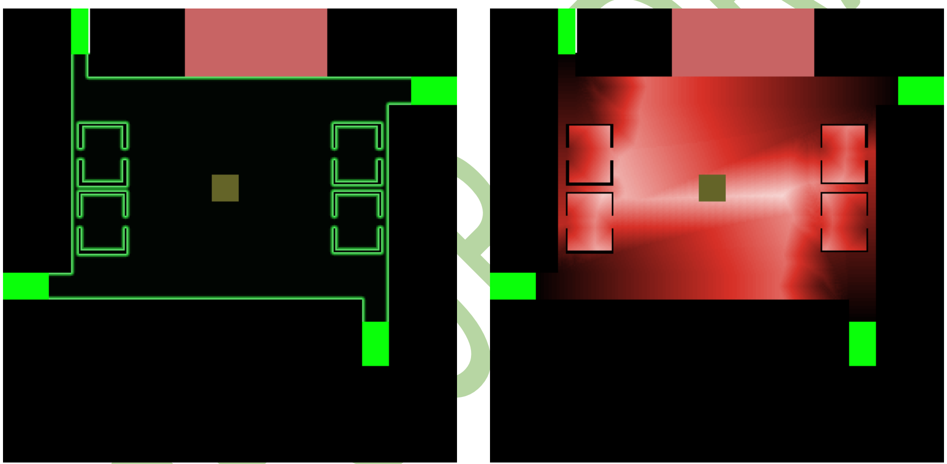

Figure 18. $P_{i,c,t}$ [-] (right – red for higher repulsion, black for no repulsion) and $F_{d,c,t}$ [-] (left – white to red to black for increasing distance attraction) visualization for the BET3 scenario used in preliminary simulations. Light green areas are safe areas.

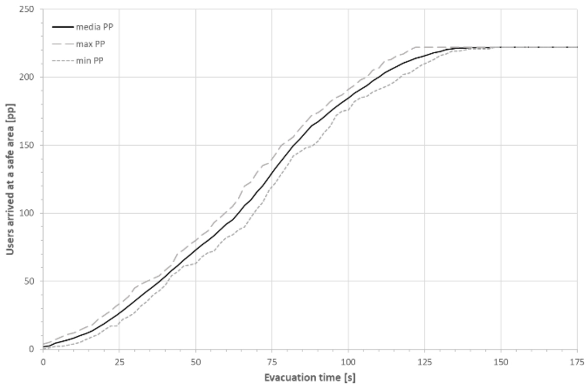

A)

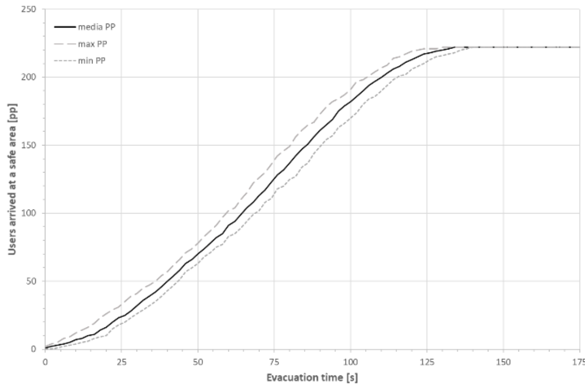

B)

Figure 19. Evacuation curve for: A) no evacuation from buildings, with only effects of $F_{d,c,t}$; B) no evacuation from buildings, but effects of $P_{i,c,t}$ (0.15) $F_{d,c,t}$ (0.7) and $OR_{c,t}$ (0.15); C)...; D)....

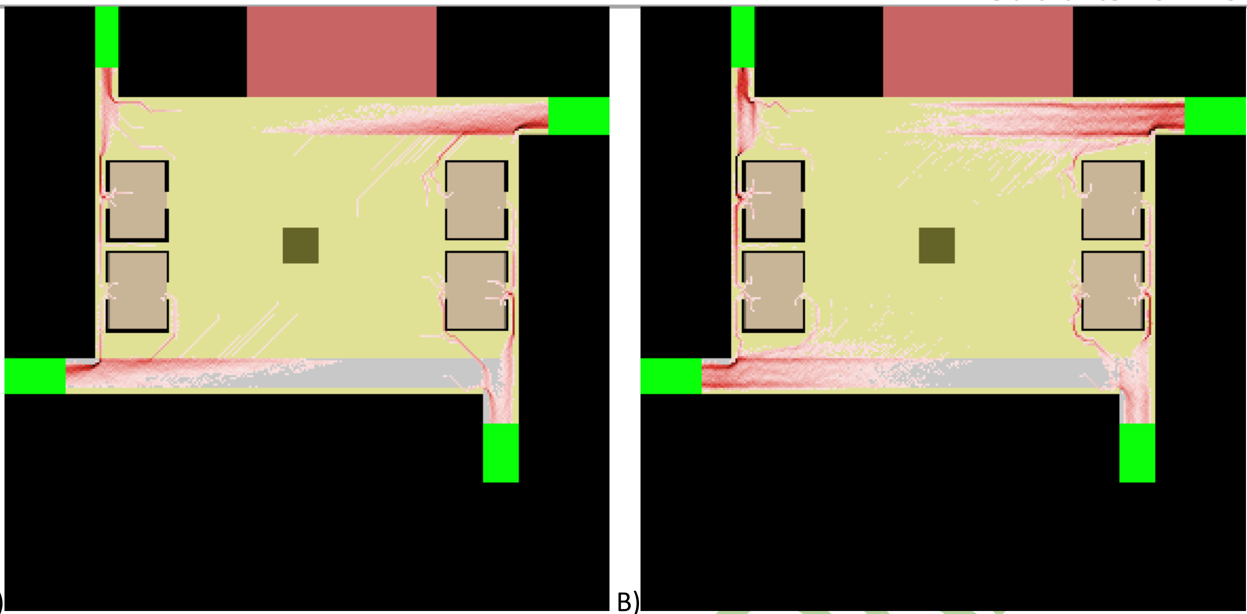
A) B)

Figure 20. Outdoor space use: A) no evacuation from buildings, with only effects of $F_{d,c,t}$; B) no evacuation from buildings, but effects of $P_{i,c,t}$ (0.15) $F_{d,c,t}$ (0.7) and $OR_{c,t}$ (0.15); C)…; D)…. Most used are in black (1, max value), less used are in white (0, not used).

Table 10. Summary of evacuation curves for condition A in Figure 19 panels

Panel	**A**
Total simulated users	**1118**
Evacuation simulation	
Max evacuating users [pp]	222
Non evacuating users [pp]	896
Users “killed” by attack [pp]	0
Max evacuation time [s]	138
Evacuation time at 95% evacuating users [s]	118
Overall flow (max) [pp/s]	1.61
Overall flow (95% users) [pp/s]	1.79
Seismic simulation:	
Density of users in the safe area [pp/m²]	0.47
Users in debris-affected area at the beginning of the simulation [pp]	1001

5. Conclusions and remarks

This report offers the development and preliminary testing of an integrated modelling methodology and software for the risk assessment in Built Environments, focused on the behaviours of their users and their interaction with the surrounding emergency conditions. The model takes advantages of different software to replicate the input conditions due to the disaster, and a netlogo model to replicate the simulation conditions under terrorist act and earthquake scenarios. The model adopts experimental-based data to represent the behaviors of users in evacuation, and also includes SLOD data (i.e. heatwave) to generate the input scenario in terms of users' presences in the open spaces depending on the UTCI levels of the different environmental patches in the square. The model can be applied to BETs - Built Environment Typologies (derived by D321) to derive typological risk conditions under certain typological (that is significant and recurring) exposure and vulnerability conditions (derived by D323). WP4-T4.2 actions will be pursued towards this end. This can speed up the risk assessment process: local authorities could directly analyse the risk level for their particular square which belongs to one of the specific BET. Then, further analysis can be also carried out in the specific reference context. In fact, it can be also used in real-world case studies, as in the aims of WP6. Further modifications could be implemented thanks to the modular structure, so as to represent other behaviours or the effects of different mitigation strategies according to WP5 actions.

6. References

Almeida JE, Kokkinogenis Z, Rossetti RJF (2012) NetLogo implementation of an evacuation scenario. Iberian Conference on Information Systems and Technologies, CISTI 1–4

Banerjee A, Maurya AK, Lämmel G (2018) Pedestrian flow characteristics and level of service on dissimilar facilities: A critical review. Collective Dynamics 3:1–52. https://doi.org/10.17815/cd.2018.17

Bernabei L, Mochi G, Bernardini G, Quagliarini E (2021a) Seismic risk of Open Spaces in Historic Built Environments: A matrix-based approach for emergency management and disaster response. International Journal of Disaster Risk Reduction 102552. https://doi.org/10.1016/j.ijdrr.2021.102552

Bernabei L, Vaiano G, Rosso F, Mochi G (2021b) A novel seismic vulnerability assessment of masonry façades: framing and validation on Caldarola case study after 2016 Central Italy Earthquake. TEMA, Technologies Engineering Materials Architecture (e-ISSN 2421-4574). https://doi.org/10.30682/tema0702i

Bernardini G, D'Orazio M, Quagliarini E (2016a) Towards a "behavioural design" approach for seismic risk reduction strategies of buildings and their environment. Safety Science 86:273–294. https://doi.org/10.1016/j.ssci.2016.03.010

Bernardini G, Ferreira TM (2020) SIMULATING TO EVALUATE, MANAGE AND IMPROVE EARTHQUAKE RESILIENCE IN HISTORICAL CITY CENTERS: APPLICATION TO AN EMERGENCY SIMULATION-BASED METHOD TO THE HISTORIC CENTRE OF COIMBRA. ISPRS - International Archives of the Photogrammetry, Remote Sensing and Spatial Information Sciences XLIV-M-1–2:651–657. https://doi.org/10.5194/isprs-archives-XLIV-M-1-2020-651-2020

Bernardini G, Lovreglio R, Quagliarini E (2019) Proposing behavior-oriented strategies for earthquake emergency evacuation: A behavioral data analysis from New Zealand, Italy and Japan. Safety Science 116:295–309. https://doi.org/10.1016/j.ssci.2019.03.023

Bernardini G, Quagliarini E, D'Orazio M (2016b) Towards creating a combined database for earthquake pedestrians’ evacuation models. Safety Science 82:77–94. https://doi.org/10.1016/j.ssci.2015.09.001

Bernardini G, Romano G, Soldini L, Quagliarini E (2021) How urban layout and pedestrian evacuation behaviours can influence flood risk assessment in riverine historic built environments. Sustainable Cities and Society 70:102876. https://doi.org/10.1016/j.scs.2021.102876

Blanco Cadena JD, Salvalai G, Lucesoli M, et al (2021) Flexible Workflow for Determining Critical Hazard and Exposure Scenarios for Assessing SLODs Risk in Urban Built Environments. Sustainability 13:4538. https://doi.org/10.3390/su13084538

Bosina E, Weidmann U (2017) Estimating pedestrian speed using aggregated literature data. Physica A: Statistical Mechanics and its Applications 468:1–29. https://doi.org/10.1016/j.physa.2016.09.044

Bunker A, Wildenhain J, Vandenbergh A, et al (2016) Effects of Air Temperature on Climate-Sensitive Mortality and Morbidity Outcomes in the Elderly; a Systematic Review and Meta-analysis of Epidemiological Evidence. EBioMedicine 6:258–268. https://doi.org/10.1016/j.ebiom.2016.02.034

Calvi GM, Pinho R, Magenes G, et al (2006) Development of seismic vulnerability assessment methodologies over the past 30 years. ISET Journal of Earthquake Technology 43:75–104

Camillen F, Caprì S, Garofalo C, et al (2009) Multi agent simulation of pedestrian behavior in closed spatial environments. In: 2009 IEEE Toronto International Conference Science and Technology for Humanity. pp 375–380

Cheunga PK, Jim CY (2019) Improved assessment of outdoor thermal comfort: 1-hour acceptable temperature range. Building and Environment 151:303–317. https://doi.org/10.1016/j.buildenv.2019.01.057

Chu ML, Law KH, Parigi P, Latombe JC (2015) Simulating individual, group, and crowd behaviors in building egress. SIMULATION 91:825–845. https://doi.org/10.1177/0037549715605363

D’Ayala D (2013) Assessing the seismic vulnerability of masonry buildings

D’Orazio M, Quagliarini E, Bernardini G, Spalazzi L (2014) EPES – Earthquake pedestrians′ evacuation simulator: A tool for predicting earthquake pedestrians′ evacuation in urban outdoor scenarios. International Journal of Disaster Risk Reduction 10:153–177. https://doi.org/10.1016/j.ijdrr.2014.08.002

Dong B, Shang C, Tong M, Cai J (2020) Analysis of the Influence of Age on Human Thermal Comfort. In: ICCREM 2020. American Society of Civil Engineers, Reston, VA, pp 170–176

FEMA-426/BIPS-06 (2011) Reference Manual to Mitigate Potential Terrorist Attacks Against Buildings. FEMA-426/BIPS-06 Edition 2 510

Ferreira TM, Vicentea R, Varum H (2014) Seismic vulnerability assessment of masonry facade walls: development, application and validation of a new scoring method. Structural Engineering and Mechanics 50:541–561. https://doi.org/10.12989/sem.2014.50.4.541

Formisano A, Florio G, Landolfo R, Mazzolani FM (2015) Numerical calibration of an easy method for seismic behaviour assessment on large scale of masonry building aggregates. Advances in Engineering Software 80:116–138. https://doi.org/10.1016/j.advengsoft.2014.09.013

French EL, Birchall SJ, Landman K, Brown RD (2019) Designing public open space to support seismic resilience: A systematic review. International Journal of Disaster Risk Reduction 34:1–10. https://doi.org/10.1016/j.ijdrr.2018.11.001

Gayathri H, Aparna PM, Verma A (2017) A review of studies on understanding crowd dynamics in the context of crowd safety in mass religious gatherings. International Journal of Disaster Risk Reduction 25:82–91. https://doi.org/10.1016/J.IJDRR.2017.07.017

Guy S, Chhugani J, Curtis S, et al (2010) Pledestrians: a least-effort approach to crowd simulation. In: ACM SIGGRAPH Symposium on Computer Animation. The Eurographics Association

Hartson HR (2003) Cognitive, physical, sensory, and functional affordances in interaction design. Behaviour and Information Technology 22:315–338. https://doi.org/10.1080/01449290310001592587

Hassanpour S, Rassafi AA (2021) Agent-Based Simulation for Pedestrian Evacuation Behaviour Using the Affordance Concept. KSCE Journal of Civil Engineering 25:1433–1445. https://doi.org/10.1007/s12205-021-0206-7

Helbing D, Molnár P (1995) Social force model for pedestrian dynamics. Physical Review E

Hissel F, Morel G, Pescaroli G, et al (2014) Early warning and mass evacuation in coastal cities. Coastal Engineering 87:193–204. https://doi.org/10.1016/j.coastaleng.2013.11.015

Italian Government (1996) DM 19/08/1996: Fire safety criteria for entertainment public spaces (Regola tecnica di prevenzione incendi per la progettazione, costruzione ed esercizio dei locali di intrattenimento e di pubblico spettacolo)

Jamei E, Rajagopalan P, Seyedmahmoudian M, Jamei Y (2016) Review on the impact of urban geometry and pedestrian level greening on outdoor thermal comfort. Renewable and Sustainable Energy Reviews 54:1002–1017. https://doi.org/10.1016/j.rser.2015.10.104

Ji Q, Gao C (2007) Simulating crowd evacuation with a leader-follower model. International Journal of Computer Sciences and Engineering Systems 1:249–252

Kenney WL, Munce TA (2003) Invited Review: Aging and human temperature regulation. Journal of Applied Physiology 95:2598–2603. https://doi.org/10.1152/japplphysiol.00202.2003

Kuligowski ED (2016) Computer Evacuation Models for Buildings. In: SFPE Handbook of Fire Protection Engineering. Springer New York, New York, NY, pp 2152–2180

Lakoba TI, Kaup DJ, Finkelstein NM (2005) Modifications of the Helbing-Molnár-Farkas-Vicsek Social Force Model for Pedestrian Evolution. Simulation. https://doi.org/10.1177/0037549705052772

Li Piani T (2018) Progettazione strutturale e funzione sociale dello spazio (quale) vulnerabilità e soluzione al terrorismo urbano. Sicurezza, terrorismo e società - INTERNATIONAL JOURNAL - Italian Team for Security, erroristic Issues & Managing Emergencies (in italian; ISSN: 2421-4442) 7–15

Li R, Klippel A (2016) Wayfinding Behaviors in Complex Buildings. Environment and Behavior 48:482–510. https://doi.org/10.1177/0013916514550243

Li S, Yu X, Zhang Y, Zhai C (2018) A numerical simulation strategy on occupant evacuation behaviors and casualty prediction in a building during earthquakes. Physica A: Statistical Mechanics and its Applications 490:1238–1250. https://doi.org/10.1016/j.physa.2017.08.058

Liu Q (2018) A social force model for the crowd evacuation in a terrorist attack. Physica A: Statistical

Mechanics and its Applications. https://doi.org/10.1016/j.physa.2018.02.136

Liu R, Jiang D, Shi L (2016) Agent-based simulation of alternative classroom evacuation scenarios. Frontiers of Architectural Research 5:111–125. https://doi.org/10.1016/j.foar.2015.12.002

Lumbroso D, Davison M (2018) Use of an agent-based model and Monte Carlo analysis to estimate the effectiveness of emergency management interventions to reduce loss of life during extreme floods. Journal of Flood Risk Management 11:S419–S433. https://doi.org/10.1111/jfr3.12230

Mas E, Adriano B, Koshimura S (2013) An integrated simulation of tsunami hazard and human evacuation in La Punta, Peru. Journal of Disaster Research 8:285–295

Mayzner MS, Shaw R, Bransford J (1978) Perceiving, Acting, and Knowing: Toward an Ecological Psychology. In: The American Journal of Psychology. p 155

Nasir M, Lim CP, Nahavandi S, Creighton D (2014) Prediction of pedestrians routes within a built environment in normal conditions. Expert Systems with Applications 41:4975–4988. https://doi.org/10.1016/j.eswa.2014.02.034

Opper S, Cinque P, Davies B (2010) Timeline modelling of flood evacuation operations. Procedia Engineering 3:175–187. https://doi.org/10.1016/j.proeng.2010.07.017

Paolini R, Mainini AG, Poli T, Vercesi L (2014) Assessment of Thermal Stress in a Street Canyon in Pedestrian Area with or without Canopy Shading. Energy Procedia 48:1570–1575. https://doi.org/10.1016/j.egypro.2014.02.177

Parisi DR, Dorso CO (2005) Microscopic dynamics of pedestrian evacuation. Physica A: Statistical Mechanics and its Applications 354:606–618. https://doi.org/10.1016/j.physa.2005.02.040

Pluchino S, Tribulato CMG, Caverzan A, et al (2015) Agent-Based Model for Pedestrians ' Evacuation after a Blast Integrated with a Human Behavior Model. In: Structures Congress 2015. ASCE, pp 1506–1517

Quagliarini E, Fatiguso F, Lucesoli M, et al (2021a) Risk Reduction Strategies against Terrorist Acts in Urban Built Environments: Towards Sustainable and Human-Centred Challenges. Sustainability 13:901. https://doi.org/10.3390/su13020901

Quagliarini E, Lucesoli M, Bernardini G (2021b) How to create seismic risk scenarios in historic built environment using rapid data collection and managing. Journal of Cultural Heritage 48:93–105. https://doi.org/10.1016/j.culher.2020.12.007

Ronchi E, Kuligowski ED, Peacock RD, Reneke P a. (2014) A probabilistic approach for the analysis of evacuation movement data. Fire Safety Journal 63:69–78. https://doi.org/10.1016/j.firesaf.2013.11.012

Ronchi E, Nilsson D, Nilsson D (2013) The Process of Verification and Validation of Building Fire Evacuation Models NIST Technical Note 1822 The Process of Verification and Validation of Building Fire Evacuation Models

Russo M, Angelosanti M, Bernardini G, et al (2020) Morphological systems of open spaces in built environment prone to Sudden-onset disasters. In: International Conference on Sustainability in Energy and Buildings SEB 2020. Split, Croatia, pp 1–10

Salecker J, Sciaini M, Meyer KM, Wiegand K (2019) The nlrx r package: A next-generation framework for reproducible NetLogo model analyses. Methods in Ecology and Evolution 10:1854–1863. https://doi.org/10.1111/2041-210X.13286

Sarmady S, Haron F, Talib A (2014) Simulation of Pedestrian Movements Using Fine Grid Cellular Automata Model. arXiv preprint arXiv:14063567

Sharifi A (2019a) Resilient urban forms: A review of literature on streets and street networks. Building and Environment 147:171–187. https://doi.org/10.1016/j.buildenv.2018.09.040

Sharifi A (2019b) Urban form resilience: A meso-scale analysis. Cities 93:238–252. https://doi.org/10.1016/j.cities.2019.05.010

Sharifi E, Lehmann S (2015) Correlation analysis of surface temperature of rooftops, streetscapes and urban heat island effect: Case study of central Sydney. Journal of Urban and Environmental Engineering 9:3–11. https://doi.org/10.4090/juee.2015.v9n1.003011

Shi L, Xie Q, Cheng X, et al (2009) Developing a database for emergency evacuation model. Building and Environment 44:1724–1729. https://doi.org/10.1016/j.buildenv.2008.11.008

Shrestha SR, Sliuzas R, Kuffer M (2018) Open spaces and risk perception in post-earthquake Kathmandu city. Applied Geography 93:81–91. https://doi.org/10.1016/J.APGEOG.2018.02.016

Simeone D, Coraglia UM, Cursi S, Fioravanti A (2016) Behavioural Simulation for Built Heritage Use Planning. 34th International Conference on Education and research in Computer Aided Architectural Design in Europe, Oulu 503–510

van der Wal CN, Formolo D, Robinson MA, et al (2017) Simulating crowd evacuation with socio-cultural, cognitive, and emotional elements. Lecture Notes in Computer Science (including subseries Lecture Notes in Artificial Intelligence and Lecture Notes in Bioinformatics) 10480 LNCS:139–177. https://doi.org/10.1007/978-3-319-70647-4_11

van der Wal CN, Formolo D, Robinson MA, Gwynne S (2021) Examining Evacuee Response to Emergency Communications with Agent-Based Simulations. Sustainability 13:4623. https://doi.org/10.3390/su13094623

van Hoof J, Schellen L, Soebarto V, et al (2017) Ten questions concerning thermal comfort and ageing. Building and Environment 120:123–133. https://doi.org/10.1016/j.buildenv.2017.05.008

Villagràn De León JC (2006) Vulnerability: A conceptual and methodological review

Wilensky U (1999) NetLogo. http://ccl.northwestern.edu/netlogo/. In: Center for Connected Learning and Computer-Based Modeling, Northwestern University, Evanston, IL

Wilensky U, Rand W (2015) An introduction to agent-based modeling. Modeling Natural, Social, and Engineered Complex Systems with NetLogo. MIT Press

Zipf GK (1950) Human behavior and the principle of least effort. Journal of Clinical Psychology 6:306. https://doi.org/10.1002/1097-4679(195007)6:3<306::AID-JCLP2270060331>3.0.CO;2-7

Zlateski A, Lucesoli M, Bernardini G, Ferreira TM (2020) Integrating human behaviour and building vulnerability for the assessment and mitigation of seismic risk in historic centres: Proposal of a holistic human-centred simulation-based approach. International Journal of Disaster Risk Reduction 43:101392. https://doi.org/10.1016/j.ijdrr.2019.101392

7. Appendix A: ABM model for users' setup and simulation schemes in the SLOD and SLOT-to-SUOD process

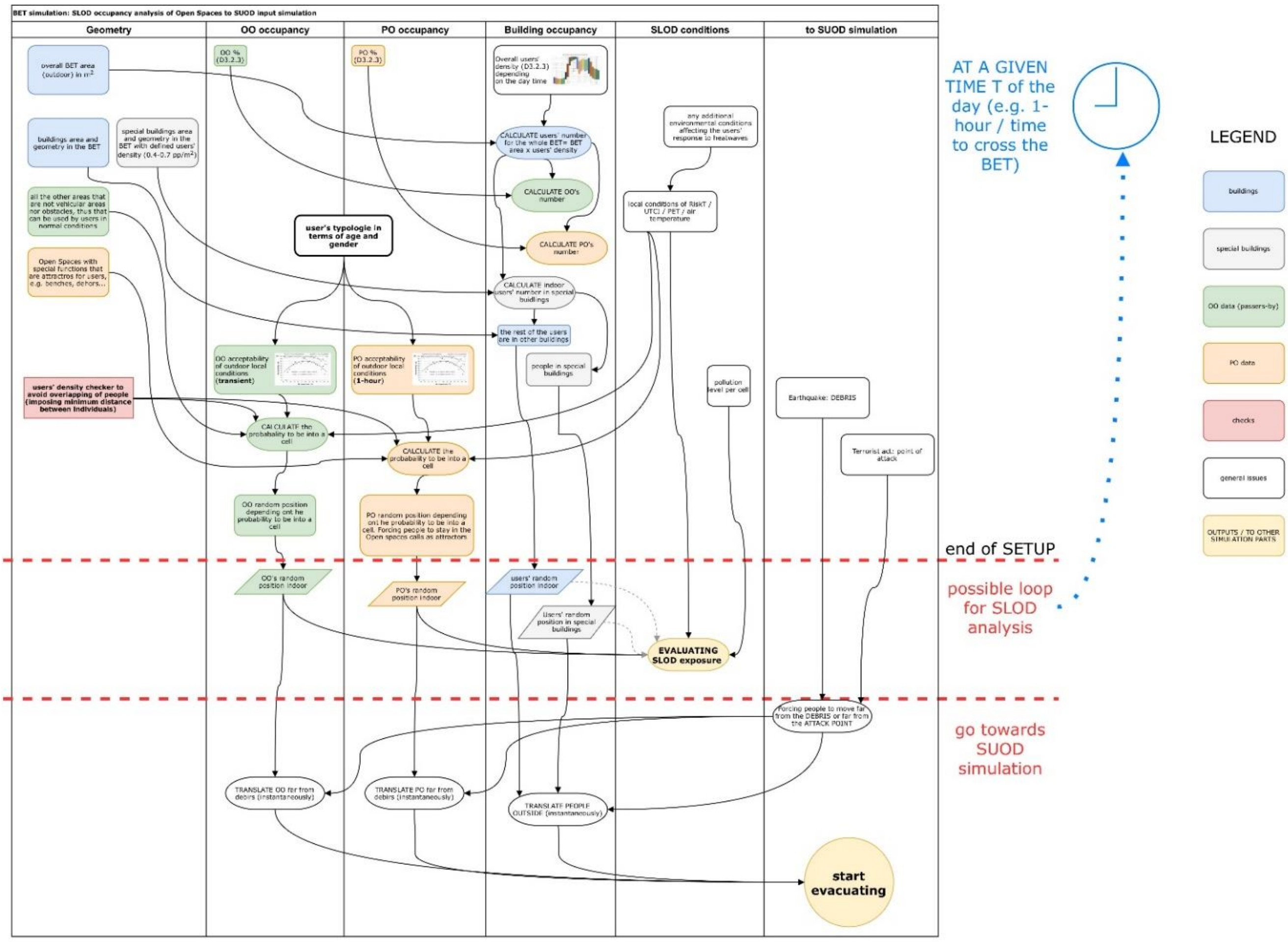

8. Appendix B: Debris assessment for all the BETs